

Università degli Studi di Salerno

Dipartimento di Chimica e Biologia “Adolfo Zambelli”



PhD Course in Chemistry

XXXI Cycle

**CATALYSIS FOR THE
TRANSFORMATION OF BIOMASS
IN VALUE-ADDED PRODUCTS**

PhD Student: *Maria Ricciardi*

Supervisor: *Prof. Antonio Proto*

Co-Supervisor: *Prof. Carmine Capacchione*

External Supervisor: *Prof. Fabrizio Passarini*

PhD Course Coordinator: *Prof. Gaetano Guerra*

Academic year 2017-2018

Abstract

The present doctoral thesis is focused on the catalytic conversion of bio-glycidol into value-added products.

Bio-glycidol (2,3-epoxy-1-propanol) is obtained from 2-chloro-1,3-propanediol, produced as waste during the Epicerol® process, that represents one of the most consolidated bio-based industrial process able to convert glycerol into epichlorohydrin.

Glycidol, in turn, is successfully employed as starting material to produce glyceryl ethers, propanediols and glycerol ketals.

Homogeneous and heterogeneous Lewis and Brønsted acids were used as catalysts for the etherification of glycidol by ring opening reaction with an alcohol as nucleophile.

As a matter of fact, commercial metal salts (chlorides and triflates of Fe, Al, Bi and Zn) were tested as homogeneous catalysts giving promising results in term of the catalytic activity in the case of metal triflates.

Moreover, a Fe(III) triflate complex bearing and [OSSO]-type ligand was synthesized and used as catalyst to enhance the regioselectivity of the reaction.

Moving to heterogeneous catalysts, sulfonated resins, metal triflates and sulfonic groups supported catalysts were employed in the synthesis of glycerol monoethers, achieving good results.

The proposed synthetic route can be applied to several alcoholic substrates ranging from short chain to long chain alcohols, obtaining precious compounds in high yield.

Considering the hydrogenolysis reaction of glycidol, instead, a system formed by the combination of Amberlyst 15 and palladium on carbon was used as catalyst. An acid resin such as Amberlyst 15 can act as co-catalyst in the hydrogenolysis thanks to its property to activate the epoxide ring

towards the ring opening reaction. The amount of this resin and the solvent medium were optimized in order to reach total selectivity towards 1,2-propanediol.

Lastly, several acid heterogeneous catalysts, both commercially available and synthetic, were tested in the ketalization reaction of glycidol with acetone, producing solketal under mild reaction conditions.

The best catalytic system, under optimized conditions, was selected for the production of other glycerol ketals using different ketones as starting material.

Furthermore, life cycle assessment (LCA) analyses, performed in collaboration with Doctor Daniele Cespi and Professor Fabrizio Passarini, were used as a tool to evaluate the environmental sustainability of the proposed synthetic processes, comparing them with those reported in literature.

Summary

Abstract	I
GENERAL INTRODUCTION	1
Biomasses conversion and glycerchemistry	1
Aim of the PhD Project	5
1 GLYCIDOL AS VALUABLE FEEDSTOCK FOR CHEMICALS PRODUCTION	7
1.1 Glycidol properties and applications	7
1.2 Industrial preparation of glycidol and development of new bio- based alternatives	8
1.3 Conversion of glycidol to value-added products	9
1.4 Glycidol derivates: synthesis and applications	13
1.4.1 Glyceryl ethers	13
1.4.2 Propanediols	19
1.4.3 Glycerol ketals	22
1.5 References	25
2 MATERIALS AND METHODS	29
2.1 Materials	29
2.2 Catalysts synthesis	30
2.2.1 Synthesis of metal triflate supported catalysts	30
2.2.2 Synthesis of sulfonated catalysts	30
2.2.3 Synthesis of [OSSO]-Iron(III) triflate complex	31

2.3 Catalysts characterization	32
2.3.1 Total acidity and BET surface area of heterogeneous acid catalysts.....	32
2.3.2 Metal content and infrared spectra of triflates supported catalysts.....	32
2.3.3 X-ray diffraction and photoelectron spectroscopy of Pd/C-A15 system	33
2.3.4 Transmission electron microscopy of Pd/C-A15 system.....	33
2.3.5 Morphological and elemental analysis of Pd/C-A15 system.....	34
2.3.6 NMR of [OSSO]-Iron(III) triflate complex	34
2.4 Experimental procedures	34
2.4.1 Recovery of 2-chloro-1,3-propanediol from chlorination mixture	34
2.4.2 Glycidol synthesis from monochlorohydrins	35
2.4.3 Glyceryl ethers synthesis	35
2.4.4 Propanediols synthesis	36
2.4.5 Glycerol ketals synthesis.....	36
2.5 Compounds analysis and quantification	37
2.6 Life cycle assessment (LCA) methodology	38
2.7 Density functional theory (DFT) calculations.....	39
2.8 References.....	40
3 RESULTS AND DISCUSSION	42
3.1 Glycidol production form Epicerol® waste	42
3.2 General properties of the catalysts	45

3.2.1 Total acidity and BET surface area	45
3.2.2 Metal content and type of surface acidity	46
3.2.3 [OSSO]-Iron(III) triflate complex	49
3.3 Glycidol etherification with alcohols	51
3.4 Etherification reactions catalysed by homogeneous catalysts	53
3.4.1. Catalytic screening of metal salts	53
3.4.2 Metal triflates as catalysts	54
3.4.2.1 Different alcoholic substrates as nucleophiles	55
3.4.2.2 Enantiopure glycidol as starting material	58
3.4.2.3 Plausible reaction mechanism.....	59
3.4.2.4 Detailed study of monobutyl glycerol ether production	60
3.4.3 [OSSO]-Iron(III) triflate complex as catalyst	63
3.4.3.1 Screening of the experimental conditions	63
3.4.3.2 Substrate scope extension.....	66
3.5 Heterogeneous catalysis for glycidol etherification.....	68
3.5.1 Catalytic screening of commercial and synthetic acid catalysts	68
3.5.2 Nafion NR 50 as efficient heterogeneous acid catalyst	72
3.5.2.1 Applicability with different alcoholic substrates.....	73
3.5.2.2 Catalyst recyclability	75
3.6 Amberlyst 15 as co-catalyst for hydrogenolysis of glycidol.....	76
3.6.1 Screening of the experimental conditions	76
3.6.2 Recyclability tests of the catalytic system	79

3.6.3 Characterization of the catalytic system after the reaction.....	80
3.6.4 Environmental considerations	85
3.7 Heterogeneous catalysis for glycidol ketalization	86
3.7.1 Screening of commercial and synthetic catalysts	86
3.7.2 Optimization of the reaction conditions with Nafion NR 50	87
3.7.3 Nafion NR 50 recyclability tests.....	89
3.7.4 Mechanistic considerations	90
3.8 References.....	96
4 CONCLUSION.....	97
ACKNOWLEDGMENTS	99
PUBLICATIONS ON THE PhD PROJECT.....	101
CONTRIBUTION TO CONFERENCES	102
PRIZES.....	105

GENERAL INTRODUCTION

Biomasses conversion and glycerchemistry

Over the last few years, the increasing of the price of fossil resources, their uncertain availability and environmental impacts, have forced the society to find alternative feedstocks for energy and materials production.^[1]

Thus, industrial and academic researchers have focused their attention towards the replacement of oil with biomass as raw material for chemical production.^[2-4]

Indeed, it was developed the concept of biorefinery, as a facility that involves the separation of biomass sources into their building blocks (triglycerides, carbohydrates, proteins, and so on) and the conversion of them into biofuels, energy and chemicals.

As a matter of fact, the use of renewable feedstock is one of the most important points to make chemical reactions in line with the twelve fundamental principles of Green Chemistry.^[5] This discipline, actually, promotes “the efficient use of raw materials, preferably renewable, eliminates waste and avoids the use of toxic and/or hazardous reagents and solvents in the manufacture and application of chemical products”.^[6] Moreover, the methods and techniques employed must minimize environmental impacts.

In this scenario the main bio-based feedstocks are triglycerides, carbohydrates, lignin and mixed organic residues (compost, biogas residues, wood ash, sewage sludge).

Triglycerides derived from vegetable oils are nowadays employed for biodiesel production through transesterification with an alcohol, usually methanol. During this reaction, glycerol (1,2,3-propanetriol) is recovered as main by-product.

Moreover, this compound is also obtained as waste in other bio-based processes, e. g. saponification of vegetable oil, as shown in Figure 1.

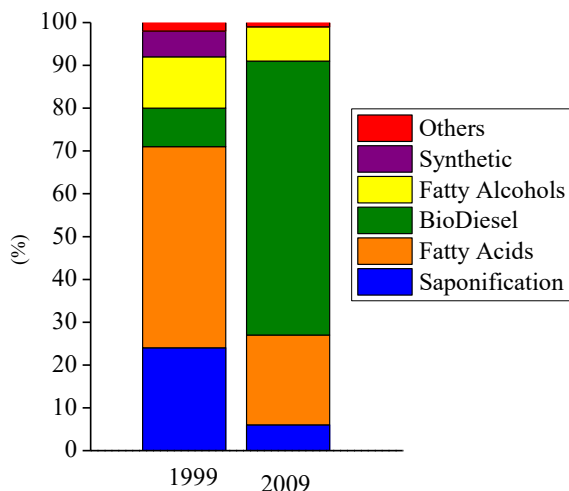


Figure 1. Glycerol production in 1999 and 2009.^[7]

Notably, until 1999 glycerol was mainly produced by the oleochemicals industry. Nowadays, due to the continuous increase of the biodiesel demand, the main provider of glycerol is the biodiesel industry (28 billion L produced in 2017^[8]). Consequently, significant amounts of glycerol have been put on the market and in 2020 its production is expected to rise to 2.5 Mt, with an expected income of \$ 2.1 billion.^[9]

For these reasons glycerol was recently recognised as renewable feedstock for chemical production, and the term “glycerochemistry” was used by the scientists to indicate the conversion of glycerol into different chemical products (Figure 2).^[2,9]

Selective oxidation of glycerol leads to commercially useful compounds and important fine chemicals such as tartronic acid, glyceraldehyde and dihydroxyacetone.^[10] Acrolein can be obtained from glycerol in excellent yield by using a method based on glycerol dehydration on acidic solid

catalysts at 250-340 °C. Moreover, to produce syngas, instead, glycerol must be treated at 225-300 °C in aqueous phase using a platinum-based catalyst.^[11]

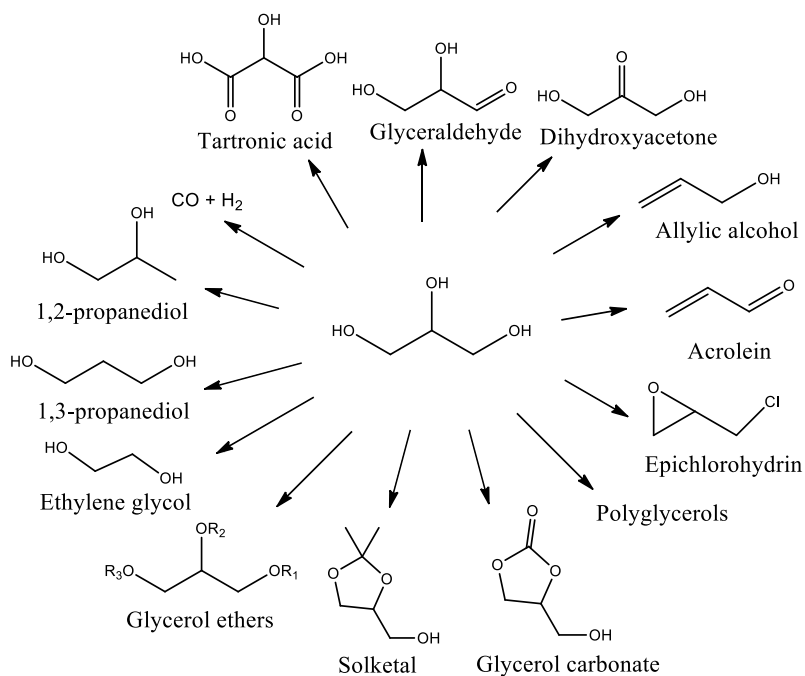


Figure 2. Glychochemistry: glycerol conversion to value-added products.

Among all the glycerol-based routes, the production of epichlorohydrin from glycerol (the so-called Epicerol® process) was implemented into an industrial process, as a greener alternative to the fossil-based process that involves the chlorination of propene at elevated temperatures.^[12]

The Epicerol® process, started in 2011 by Solvay, consists in the reaction of glycerol with gaseous hydrochloric acid (2 equivalents) in the presence of carboxylic acid as Lewis acid catalysts followed by elimination under basic conditions (Figure 3).

During the first step of glycerol chlorination, 3-chloro-1,2-propanediol (or 1-monochlorohydrin) and water are formed together with a tiny quantity of

2-chloro-1,3-propanediol (or 2-monochlorhydrin). The second chlorination step leads to the formation of 1,3-dichloro-2-propanol and a small amount of 1,2-dichloropropanol.^[13]

In the final step of the process, 1,3-dichloro-2-propanol reacts with sodium hydroxide to form epichlorohydrin.

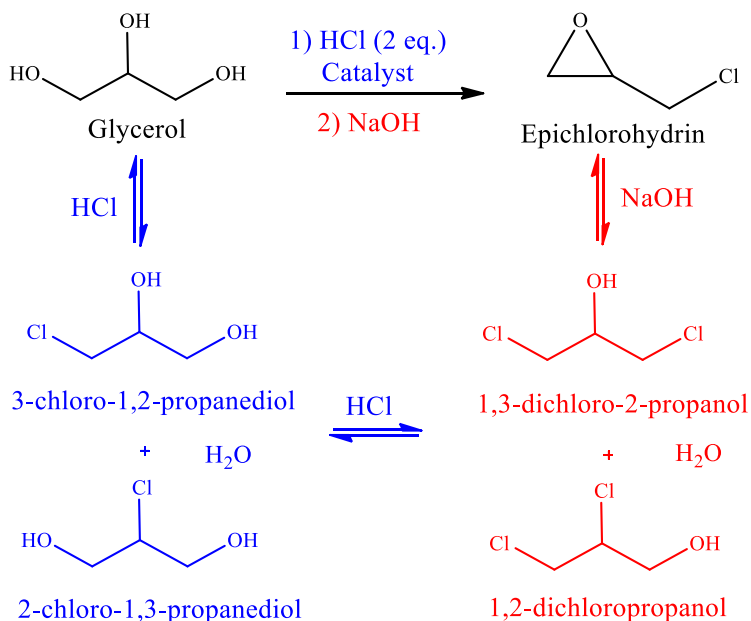


Figure 3. Epichlorohydrin production from glycerol (Epicerol® process).

It is worth noting that 2-chloro-1,3-propanediol does not undergo further chlorination because the β position inhibits the reaction, leaving this compound as the main waste of the overall process (7.5 % in moles).

So, new pathways for the recovery and the conversion of 2-chloro-1,3-propanediol into value-added products are worth to be investigated to make the Epicerol® process even more sustainable.

Aim of the PhD Project

The PhD project is based on the preparation of glycidol from Epicerol® process wastes and its further conversion into value-added products such as glyceryl ethers, propanediols and glycerol ketals (Figure 4).

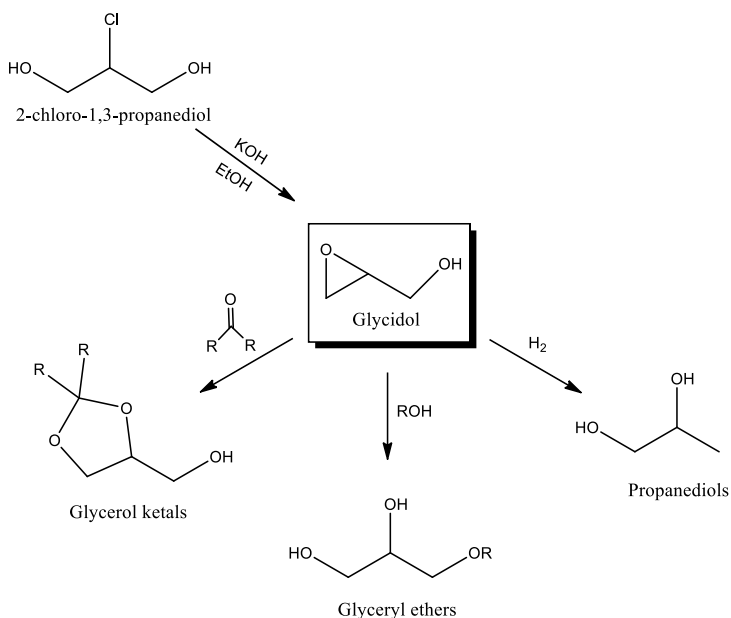


Figure 4. Scheme of the reactions investigated during the PhD project.

The synthesis of glyceryl ethers was performed for the first time through ring opening reaction of glycidol with alcohols in the presence of both homogeneous and heterogeneous acid catalysts.

A synthetic method based on the hydrogenolysis of glycidol with molecular hydrogen in the presence of palladium on carbon as catalyst and an acid resin as co-catalyst was employed to produce 1,2-propanediol.

Glycerol ketals were synthesized by using a methodology poorly investigated in literature such as the reaction of glycidol with ketones catalysed by heterogeneous catalysts.

The choice of producing these compounds comes from their important industrial applications that will be mentioned along the text.

Moreover, for all the considered processes, life cycle assessment (LCA) analyses were performed in collaboration with the research group of Professor Fabrizio Passarini in order to compare the environmental performances of the proposed routes with the traditional ones or the already reported in literature.

1 GLYCIDOL AS VALUABLE FEEDSTOCK FOR CHEMICALS PRODUCTION

1.1 Glycidol properties and applications

Glycidol or 2,3-epoxy-1-propanol is an epoxide alcohol that is a colourless liquid, miscible with water, alcohols, esters, ketones, ethers, and aromatics and almost insoluble in aliphatic hydrocarbons.^[14]

Thanks to contemporary presence of the oxiranic and the alcoholic functionalities, it is a very reactive compound. In fact, it may decompose once exposed to moisture and oligomerise at temperatures higher than 90 °C.^[15] Moreover, glycidol is an irritant and toxic compound, classified as a carcinogenic substance since 1994.^[16]

Due to its high reactivity, it must be stored at 2-8 °C and distilled prior to being used under inert atmosphere.

Before 1970s, it was used only for research purposes, after that it was widely employed in pharmaceutical industry. In fact, as pure enantiomer, it is an important intermediate in the industrial synthesis of biologically active compounds and pharmaceutical products as well as in the production of insecticides and sweetening and flavouring agents.^[17]

Furthermore, this compound is employed as alkylating agent, emulsion breaker, dye-levelling agent, and stabilizer in the manufacture of natural oils and polymers.

1.2 Industrial preparation of glycidol and development of new bio-based alternatives

Glycidol is currently produced at industrial level from fossil raw materials. The consolidated process consists in the oxidation of allyl alcohol (derived from propylene) with H_2O_2 catalysed by titanium silicate (TS-1). Under these conditions, a glycidol yield of 40 % was attained due to the low conversion of allyl alcohol (47 %) and the high selectivity (92.5 %).^[18,19]

In literature, different examples are reported to prepare glycidol, alternative to the industrial one as shown in Figure 5.

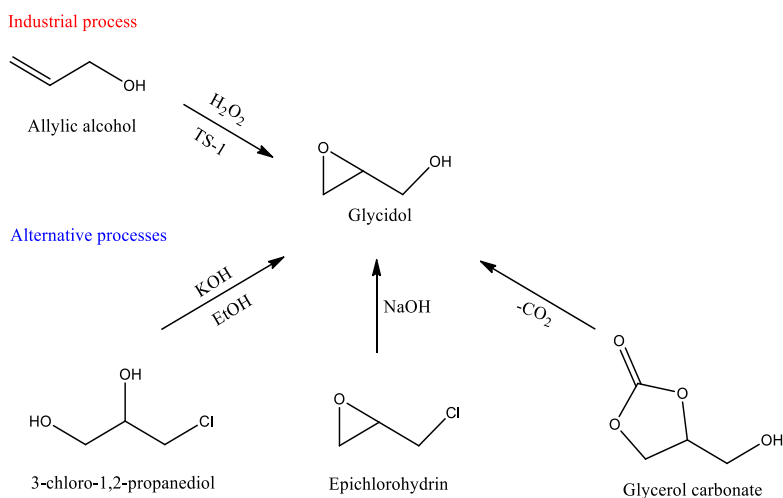


Figure 5. Glycidol synthesis: comparison of industrial process and alternatives ones.

The basic treatment (with KOH or NaOH) of chlorinated compounds such as 3-chloro-1,2-propanediol^[20] and epichlorohydrin^[21] produces glycidol through a classic organic reaction while the decomposition of glycerol carbonate and the catalytic transesterification of glycerol with dimethylcarbonate has been more recently investigated.^[22,23]

However, these strategies have been not implemented at industrial level probably because they are not advantageous from the economic and

environmental point of view. Therefore, a valid bio-based alternative must be found for a sustainable glycidol production.

1.3 Conversion of glycidol to value-added products

Different examples of glycidol utilization to produce value-added products are reported in literature.^[24–28]

Thanks to the fact that glycidol can easily undergo spontaneous polymerization, it was widely employed to synthesize different types of polyether polyols (polyglycerols).

The use of glycidol as a monomer is known since 1966, when Sandler and Berg^[29] firstly described its polymerization in the presence of bases.

Only twenty years later, it was discovered that branched architectures are formed through glycidol polymerization.^[30]

The polymers obtained were called hyperbranched polymers because they consist not only of branched but also linear subunits (Figure 6).

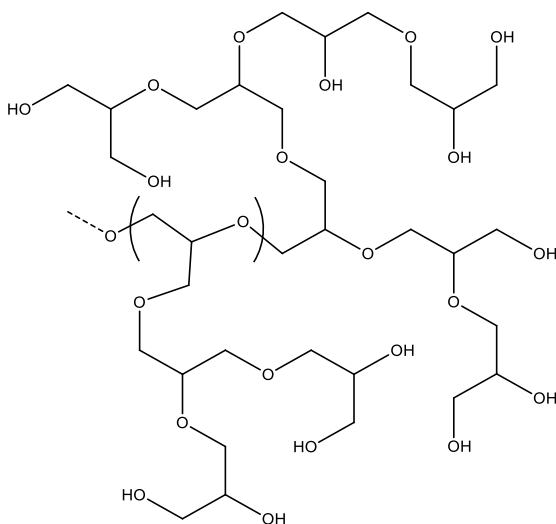


Figure 6. Structure of hyperbranched polyglycidols.

Thus, they belong to the class of dendritic molecules, useful as substitutes of dendrimers, polymers that have special properties and applications, thanks to the absence of linear units in their structure.

The increasing interest on dendritic polymers lies in the fact that they can be synthesized in a one-pot reaction within a day, while dendrimers synthesis requires a multi-step procedure.^[15]

However, the properties of the materials in the presence of linear units are quite different because the functional groups are not only placed on the surface of the molecule. Nevertheless, if a high degree of branching is reached during their production, dendritic molecules can be successfully used in most of the applications of dendrimers.^[31,32]

Over the last 10 years, with the rising interest in hyperbranched polymers, the synthetic procedure was constantly improved by different research groups mainly following three steps:^[24]

- a. Deprotonation of the initiator;
- b. Slow monomer (glycidol) addition to the reactor at a fixed temperature;
- c. Deactivation of the final mixture using a cationic ion exchange resin.

By using these methods, polyglycerols with a highly flexible aliphatic polyether backbone and numerous hydroxyl end groups are formed.^[30]

The presence of such hydroxyl end groups gives to this material a good water solubility and an excellent biocompatibility that makes it suitable for the use as scaffold in the synthesis of nanocapsules, soluble catalysts support, protein-resistant surfaces, and in polymer-based therapies and diagnostics.^[24,33]

Moving to pharmaceutical compounds, drugs such as mephenesin^[34] (3-(2-methylphenoxy)-1,2-propanediol) and guaifenesin^[35] (3-(2-methoxyphenoxy)-1,2-propanediol) can be synthesized from glycidol through ring opening reaction with *ortho*-substituted phenols (Figure 7).

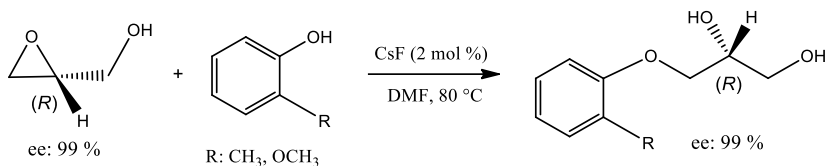


Figure 7. Mephesisin and guaifenesin production from glycidol.

High yields (around 91-92 %) were achieved after 6-9 h of reaction at 80 °C in the presence of CsF (2 % in moles) as catalyst.^[28]

Recently, glycidol was employed in the synthesis of glycerol carbonate through the reaction of the epoxide ring with carbon dioxide (Figure 8).^[36]

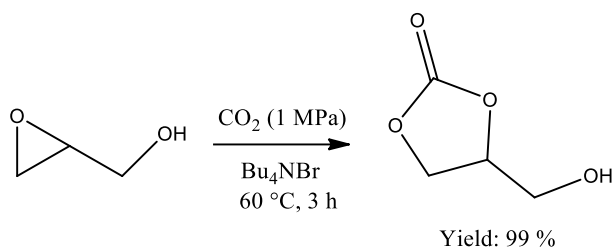
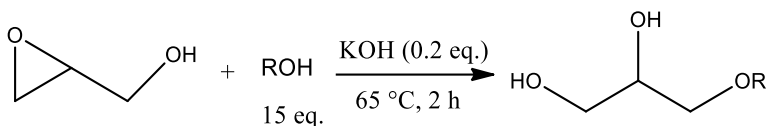


Figure 8. Glycerol carbonate synthesis from glycidol.

Thanks to glycidol reactivity, the product is obtained in high yield under mild reaction conditions in the presence of tetra-alkyl ammonium salt without the need of a metal catalyst.

In 2017, the etherification of glycidol with alcohols under basic conditions^[25] was reported by the research group of A. Leal-Duaso. Slow addition of glycidol to the reaction medium and high catalyst loading (20 % in moles respect to glycidol) are needed to reach from poor to excellent yields depending on of the length of the alcoholic chain (Figure 9).



-R: Me, Et, *i*Pr, *n*Bu, *i*Octyl, CF₃CH₂, Ph

Yield: 22-93 %

Figure 9. Glycidol etherification under basic conditions.

In 2018, glycidol was successfully used as starting material to produce glycidyl esters.^[26] This transformation keeps the epoxydic ring intact, and can be used as an alternative method for the production of glycidyl compounds, employed as monomers for functional epoxy resins.^[37]

Glycidyl esters are obtained through transesterification of methyl esters with glycidol in the presence of quaternary alkyl ammonium salt (Figure 10).

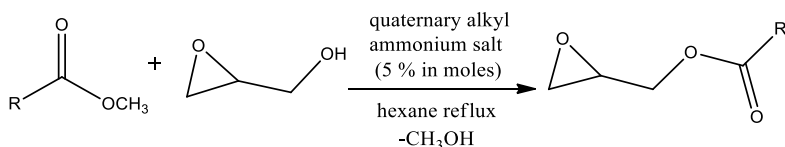


Figure 10. Reaction scheme for glycerol esters synthesis from glycidol.

The alkyl ammonium cation interacts with epoxide ring of glycidol, inhibiting the undesired ring opening polymerization and favouring the transesterification reaction. By using this strategy, different functional compounds and materials containing epoxy moieties can be easily synthesized from glycidol.

Therefore, the interest towards the conversion of glycidol into value-added products is increasing in the last few years.

1.4 Glycidol derivatives: synthesis and applications

1.4.1 Glycerol ethers

Glycerol ethers are chemical compounds derived from the etherification of one, two or three of alcoholic functionalities of glycerol. These compounds naturally occur as pure enantiomers in lipid membranes.^[38]

The possibility to change the alkyl chain R (branched or linear chains) of the molecule allows to develop a large class of compounds with different chemical, biological and physical properties.^[39]

As reported recently in a review by Sutter et al.^[40], the monoalkylated glycerol ethers (MAGEs) are very interesting molecules with several industrial applications in different fields ranging from cosmetics to pharmaceuticals, depending on the alkyl chain R (Figure 11).^[39,41,42]

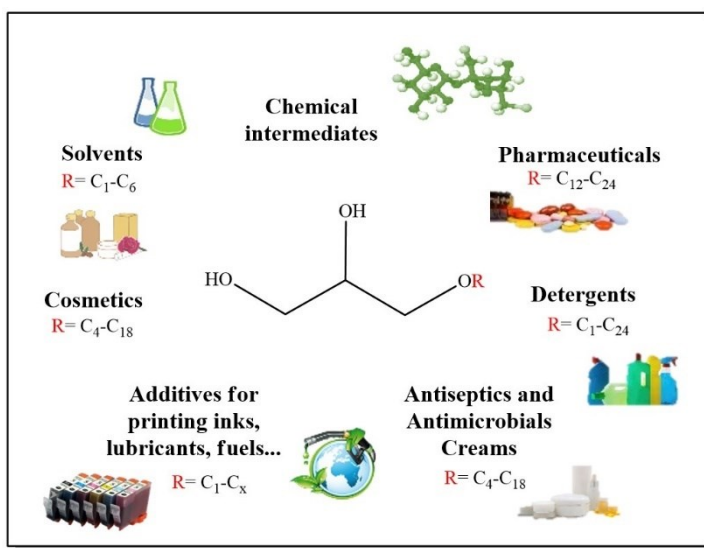


Figure 11. Glycerol ethers application fields.

Several studies have demonstrated their unique properties as surfactants, immunostimulant,^[43] antimicrobial,^[44] and antitumor activity^[45] as additives in the pharmaceutical domain, as they allow the transport of

active substances through the skin^[46] and lipid membrane^[47]. They can be found in dermatological preparations,^[48] compositions of deodorants,^[49] shampoos,^[50] and creams for the skin care^[51].

In particular, 3-[(2-ethylhexyl)oxy]-1,2-propanediol, also known as Sensiva SC50^[52], is widely used in skin creams^[40].

Most of the literature data (numerous patents) refer to studies concerning the applications of glycerol monoethers, but poor data about their production and demand are reported in literature.

All the synthetic strategies to obtain MAGEs are based on glycerol and its already known chemical intermediates (epichlorohydrin, glycidol, chloropropane diol, etc) that can be readily transformed into glycerol ethers.

The first reported synthesis of glycerol monoethers involved the SN2-type reaction of 3-chloro-1,2-propanediol with sodium alkoxide or sodium together with an excess of alcohol, in which the alkoxide substitutes the halide to form the corresponding ether (Figure 12).^[53]



Figure 12. Glyceryl ethers synthesis from 3-chloro-1,2-propanediol.

However, a dipolar aprotic solvent is needed to synthesize glycerol ether with long alkyl chains R.

Starting from epichlorohydrin, two or more steps are necessary to produce glycerol monoethers. Firstly, epichlorohydrin reacts with an alcohol under basic conditions undergoing SN2 substitution of the Cl group to form a glycidyl ether (Figure 13).

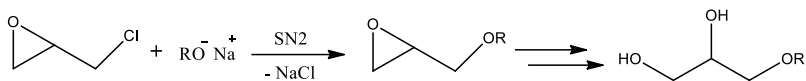


Figure 13. Glyceryl ethers synthesis from epichlorohydrin.

In this reaction, in order to reach good yields, epichlorohydrin and the base should be added in excess respect to the alcohol.^[54] Then the glycidyl ether undergoes hydrolysis reaction (generally two steps are necessary to avoid by-products) to form glycerol monoethers.

Despite the number of steps, this strategy is used by industries to prepare compounds such as Sensiva SC50 and others functionalized glycerol ethers.

The glycidyl ethers can be also prepared from glycidol (Figure 14) by the nucleophilic substitution of alkyl or aryl halide under basic conditions (Williamson-type reactions or aromatic nucleophilic substitution).^[55]

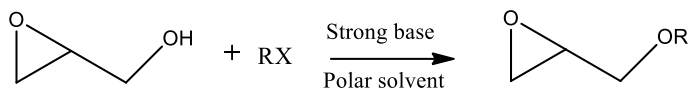


Figure 14. Glycidyl ethers synthesis from glycidol.

Furthermore, the nucleophilic addition of an alcohol on glycidol was investigated to form MAGEs via a ring-opening reaction in basic conditions^[56], observing the simultaneous formation of polyglycerols^[57]. To avoid the formation of such by-products, an excess of titanium(IV) alkoxide^[58] or aluminium derivatives (DIBAL-H)^[59] respect to glycidol must be used in alcoholic solution.

All the synthetic strategies described above suffer from the high toxicity of intermediates and reagents (epichlorohydrin, 3-chloro-1,2-propanediol, glycidyl ethers), poor atom economy and inconvenient reaction conditions (toxicity of dipolar aprotic solvents, production of salts such as metal halides).^[60]

Synthetic pathways including protection-deprotection steps starting from glycerol were employed to improve regio and chemo selectivity, but these additional steps limit their interest.

The preparation of MAGEs through direct glycerol etherification seems to be more acceptable in terms of sustainability.

However, the chemical and physical properties of glycerol (extremely hydrophilic character, three alcohol functions with similar pK_a and reactivity) make this reaction difficult and often not acceptable in the light of harsh reaction conditions needed.

Both heterogeneous and homogeneous acid catalysts are tested by several research groups in order to make efficient and selective reactions in the direct etherification of glycerol with an alcohol as alkylating agent.

However, to achieve acceptable reaction yields by using these synthetic strategy, high catalyst loading (1.7–6.5 mol %), high temperatures (150–160 °C), and long reaction times (6–24 h), are often required (Figure 15).

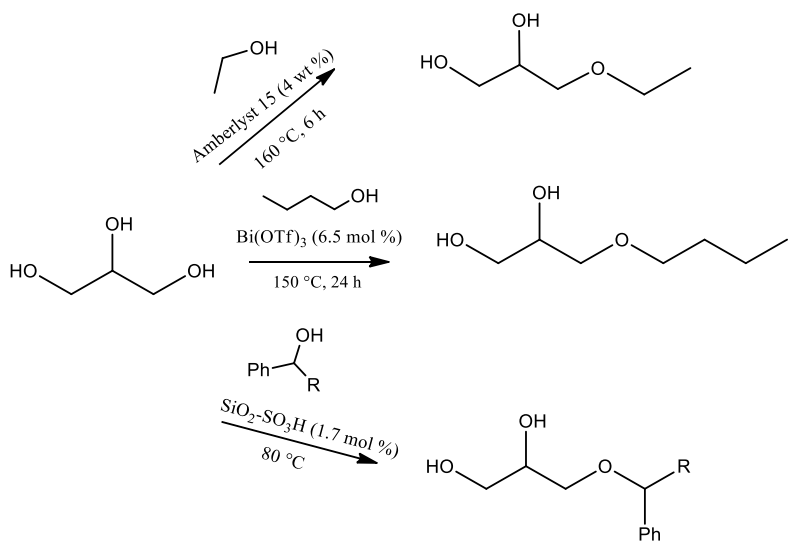


Figure 15. Different examples of glycerol ethers production from glycerol.

Using a heterogeneous catalyst, such as Amberlyst 15, ethoxy glyceryl ethers are obtained with a yield of 32 % after 6 h of the reaction between glycerol and ethanol at $160\text{ }^\circ\text{C}$.^[61]

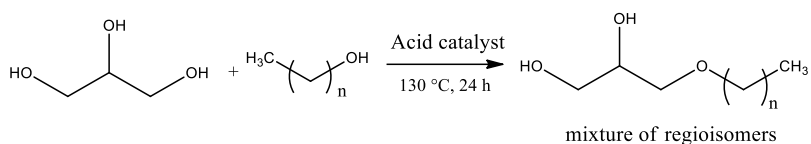
The reaction of glycerol with activated alcohols (benzylic, allylic, and propargylic, etc.) was investigated in the presence of silica-supported sulfonic groups as acid catalyst.^[62] On one hand, short reaction times (2-8 h) are necessary for secondary alcohols with an aromatic ring bonded at the α -carbon to reach good yields (70-96 %), on the other hand, longer reaction times are required for primary alcohols, such as benzyl alcohol, resulting in poor yields (61–83 %).

Finally, butoxy glyceryl ethers are obtained in 70 % yield by using a Lewis acid such as bismuth triflate as catalyst (loading of 6.5 % in moles) after 24 h of reaction at $150\text{ }^\circ\text{C}$.^[63]

Moreover, glycerol ethers with a long alkyl chain are appealing compounds thanks to their amphiphilic properties that make them suitable for applications as water-stable surfactants and solvents for catalysis. Nevertheless, their synthesis from bio-based feedstock is very complex,

delaying their industrial implementation. With the increasing of the length of the alkyl chain of the alcohols, the glycerol etherification reaction becomes more difficult because the difference in polarity between glycerol and fatty alcohols is too high, making the reaction medium biphasic. Moreover, the necessity of an excess of glycerol and high temperatures favours the formation of by-products in acidic conditions. The combination of these phenomena leads to very low reaction yields.

Lately, many attempts to find solution to these problems have been reported in literature (Figure 16).^[64,65]



$n = 11$, yield of 35 % using 0.5 eq. of H^+ and 1 eq. of CTAB

Figure 16. Reaction of long chain alcohols with glycerol.

Gaudin et al.^[65], reported that a transfer agent such as CTAB (cetyltrimethylammonium bromide) must be added to the catalytic system to allow the contact between the polar glycerol phase and the hydrophobic 1-dodecanol phase and reach acceptable reaction yields.

Therefore, innovative bio-based catalytic routes to synthesize these compounds are of great interest.

1.4.2 Propanediols

Glycerol-based diols (1,2-propanediol (1,2-PD) and 1,3-propanediol (1,3-PD)) see Figure 17 for structures) are well known compounds widely employed as commodities.^[66]

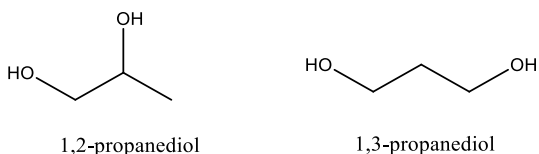


Figure 17. Propanediols structures.

Thanks to its low toxicity, 1,2 propanediol is used as a better alternative to other compounds such as ethylene glycol in food, cosmetics, detergents, paints and antifreeze liquids. Moreover, it can be used as starting material in the production of fibre manufacture, polyester resins for film, and pharmaceutical compounds.

1,3-propanediol, instead, is mainly used as monomer for the synthesis of polymers such as polyethers, polyurethanes and polytrimethylene terephthalate, a biodegradable polyester, commercially named Sorona (DuPont) or Corterra (Shell).^[67]

On the industrial scale, 1,2-propanediol is produced through a selective oxidation of propylene to propylene oxide and subsequent hydrolysis of the oxide^[68] (Figure 18) while 1,3-propanediol is catalytically obtained from ethylene oxide or acrolein (Figure 19).^[69]

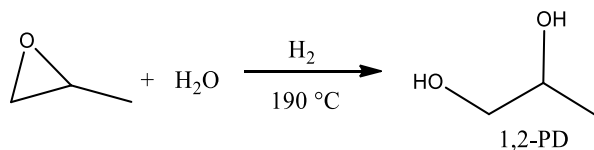


Figure 18. 1,2-propanediol synthesis from propylene oxide.

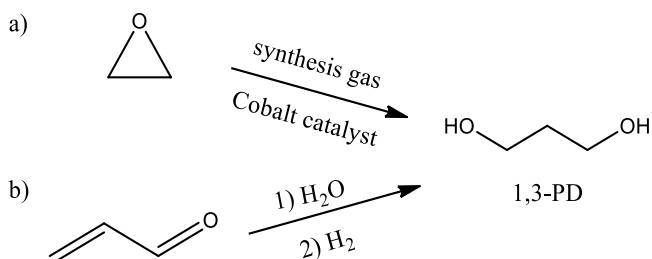


Figure 19. 1,3-propanediol synthesis: from ethylene oxide (a) and acrolein (b).

Recently, new synthetic strategies starting from biomass feedstock have been developed such as the hydrogenolysis of glycerol (Figure 20).^[66,70–72] However, this reaction requires high temperatures (130–230 °C), high hydrogen pressures (1–25 MPa), and a very selective catalyst to avoid the formation of different by-products (1-propanol, 2-propanol, ethylene glycol, and ethanol).^[73,74]

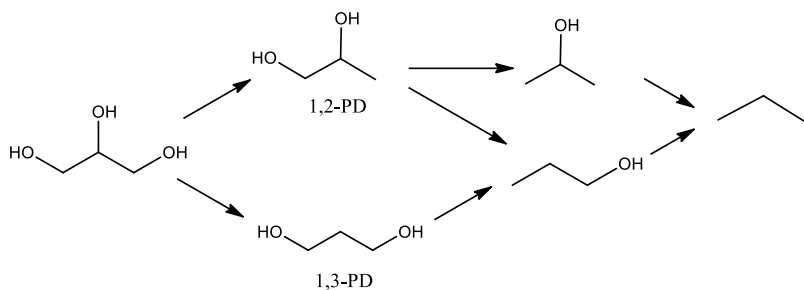


Figure 20. Glycerol hydrogenolysis products.

Notably, by using transition metal-based catalysts, glycerol undergoes a selective hydrogenolysis to 1,2-propanediol.^[75,76] A yield of 73 % of 1,2-propanediol is attained using a method based on dehydration followed by hydrogenation of glycerol over a copper chromite catalyst (CuCr₂O₄) at 200 °C and a hydrogen pressure of 10 bar coupled with a reactive distillation.^[77]

1,3-propanediol, instead, is much more difficult to be accomplished from glycerol, so far only few articles reported catalytic systems able to promote its formation with an acceptable selectivity. Only using bacterial fermentation, glycerol is selectively converted into 1,3-propanediol through an enzyme-catalysed reaction.^[78]

Very recently, glycidol hydrogenation was proposed as an alternative route to produce propanediols (Figure 21).^[27,79,80]

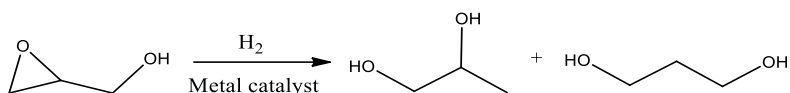


Figure 21. Propanediols synthesis from glycidol.

Depending on the catalytic system employed, the selectivity of the reaction was moved to 1,2-propanediol or 1,3-propanediol.^[27,80,81]

Performing the reaction using Ni (40 wt %) supported on an acid delaminated saponite catalysts at 180 °C, total glycidol conversion was observed after 1 h of reaction. Nevertheless, poor selectivity was reached with the formation of 29 % of 1,3-propanediol and 30 % of 1,2-propanediol.^[27] Moreover, by adding a 7 wt % of Re on the Ni catalyst at 40 wt % a selectivity towards 1,3-propanediol of 46 % was reached after 4 h of reaction at 120 °C.^[81]

Total selectivity to 1,2-propanediol was instead achieved in only 6 h of reaction at 80 °C and 8 bar of H₂ by using palladium on carbon (Pd/C) as catalyst and ethanol as solvent.^[80]

By using this strategy, propanediols were obtained under milder reaction conditions compared to those starting from glycerol.

1.4.3 Glycerol ketals

In the last decade, numerous research groups have demonstrated the potential use of oxygenated compounds like glycerol ketals as fuel additives.^[82,83]

In particular, 2,2-dimethyl-1,3-dioxolane-4-methanol (solketal) was used as flavouring agent, surfactant and biodiesel additive, reducing its viscosity and increasing its oxidation stability (Figure 22).^[84]

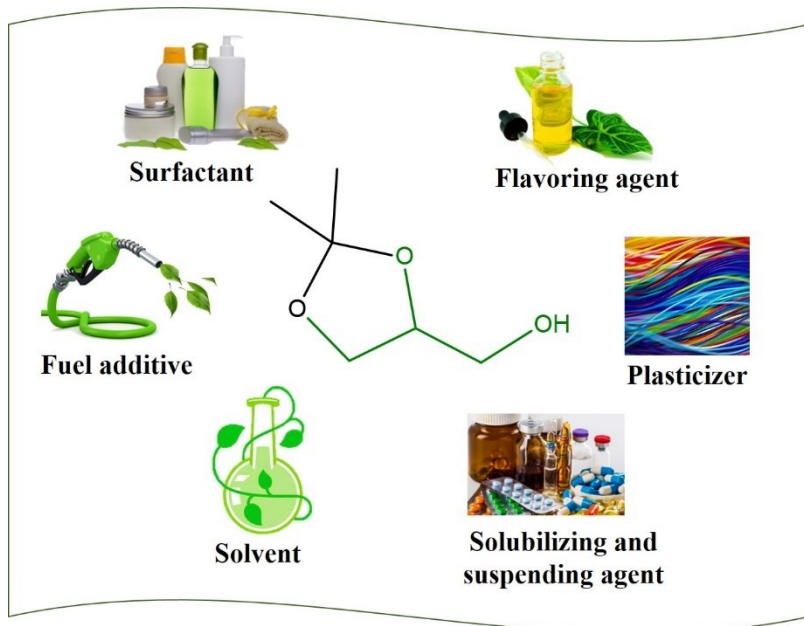


Figure 22. Typical applications of solketal.

In this field, the most pursued approach for the synthesis of solketal is the reaction of glycerol with acetone in the presence a strong homogeneous Brønsted acid catalyst usually in high loading (Figure 23).

In the last few years, several papers reported the use of heterogeneous catalysts like resins (Amberlyst type), zeolites, montmorillonite K10, sulfonated silicas, silica-supported heteropolyacids, and Lewis acids as catalysts for the conversion of glycerol to solketal.^[85]

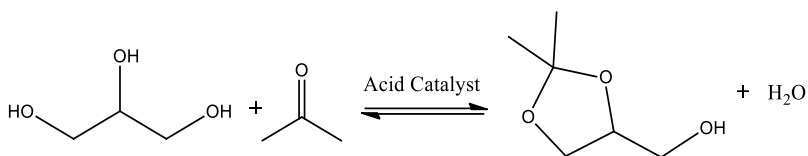


Figure 23. Synthesis of solketal from glycerol.

During this reaction, the water formed as by-product must be removed from the reaction medium to shift the chemical equilibrium towards the formation of the desired product.

In this context, glycidol can be considered a potential alternative to glycerol as starting material to produce solketal (Figure 24) avoiding the formation of water as by-product.

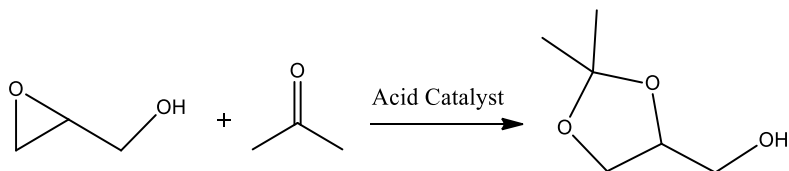


Figure 24. Synthesis of solketal from glycidol.

In spite of this advantage, only few examples of this reaction are reported in literature,^[86-88] in all the cases catalysed by homogeneous systems in high catalyst loading.

Total conversion of glycidol was reached in refluxing acetone by using a 20 % in moles of catalyst loading (2 h of reaction for RuCl_3 and 4 h of reaction for iron(III)trifluoroacetate).^[87,88]

In the presence of 1 % in moles of $\text{Er}(\text{OTf})_3$, instead, the quantitative conversion of glycidol to solketal was attained after 48 h of reaction at room temperature.^[86]

Besides, glycerol ketals such as solketal, can serve as building blocks to prepare other high-value products. In particular, through hydrogenation of the ketals in the presence of metal catalysts, monoalkyl glyceryl ethers can be easily obtained (Figure 25).^[89]

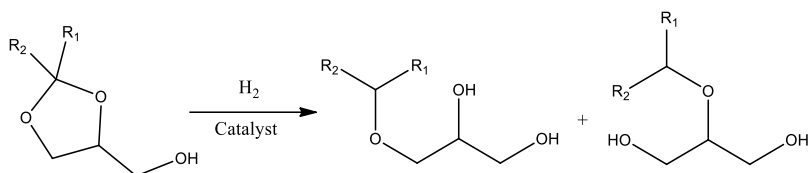


Figure 25. Synthesis of glycerol monoethers from glycerol ketals.

For example, glycerol isopropyl ether is produced with 87 % of glycerol conversion, 78 % of chemoselectivity and excellent regioselectivity between isomeric ethers at 120 °C and 20 bar of H₂ using a palladium catalyst supported on mesoporous amorphous structured aluminosilicates. Consequently, the synthesis of glycerol ketals is an active task of research.

1.5 References

- [1] F. Cherubini, *Energy Convers. Manag.* **2010**, *51*, 1412–1421.
- [2] S. Abate, P. Lanzafame, S. Perathoner, G. Centi, *ChemSusChem* **2015**, *8*, 2854–2866.
- [3] P. C. A. Bruijninx, *ChemSusChem* **2016**, *9*, 1058–1060.
- [4] M. Pagliaro, R. Ciriminna, H. Kimura, M. Rossi, C. D. Pina, *Eur. J. Lipid Sci. Technol.* **2009**, *111*, 788–799.
- [5] P. T. Anastas, J. C. Warner, *Green Chem. Theory Pract.* **1998**, 29–56.
- [6] R. A. Sheldon, *Comptes Rendus Académie Sci.-Ser. IIC-Chem.* **2000**, *3*, 541–551.
- [7] R. Ciriminna, C. D. Pina, M. Rossi, M. Pagliaro, *Eur. J. Lipid Sci. Technol.* **2014**, *116*, 1432–1439.
- [8] “Major biodiesel producing countries 2017 | Statistic,” can be found under <https://www.statista.com/statistics/271472/biodiesel-production-in-selected-countries/>, **2018**.
- [9] D. Cespi, F. Passarini, G. Mastragostino, I. Vassura, S. Larocca, A. Iaconi, A. Chierigato, J.-L. Dubois, F. Cavani, *Green Chem.* **2015**, *17*, 343–355.
- [10] M. Pagliaro, R. Ciriminna, H. Kimura, M. Rossi, C. Della Pina, *Angew. Chem. Int. Ed.* **2007**, *46*, 4434–4440.
- [11] R. R. Soares, D. A. Simonetti, J. A. Dumesic, *Angew. Chem.* **2006**, *118*, 4086–4089.
- [12] R. Vitiello, V. Russo, R. Turco, R. Tesser, M. Di Serio, E. Santacesaria, *Chin. J. Catal.* **2014**, *35*, 663–669.
- [13] R. Tesser, M. Di Serio, R. Vitiello, V. Russo, E. Ranieri, E. Speranza, E. Santacesaria, *Ind. Eng. Chem. Res.* **2012**, *51*, 8768–8776.
- [14] International Agency for Research on Cancer, Ed. , *Some Industrial Chemicals: This Publication Represents the Views and Expert Opinions of an IARC Working Group on the Evaluation of Carcinogenic Risks to Humans, Which Met in Lyon, 15 - 22 February 2000*, IARC, Lyon, **2000**.
- [15] M. E. R. Weiss, F. Paulus, D. Steinhilber, A. N. Nikitin, R. Haag, C. Schütte, *Macromol. Theory Simul.* **2012**, *21*, 470–481.
- [16] Report on Carcinogens, U.S. Department of Health and Human Services Public Health Service National Toxicology Program, Twelfth Edition, **2011**, pp 215.
- [17] R. M. Hanson, *Chem. Rev.* **1991**, *91*, 437–475.
- [18] L. Harvey, E. Kennedy, B. Z. Dlugogorski, M. Stockenhuber, *Appl. Catal. Gen.* **2015**, *489*, 241–246.
- [19] A. Wróblewska, A. Fajdek, *J. Hazard. Mater.* **2010**, *179*, 258–265.
- [20] T. H. Rider, A. J. Hill, *J. Am. Chem. Soc.* **1930**, *52*, 1521–1527.
- [21] K. Weissermel, H.-J. Arpe, in *Ind. Org. Chem.*, Wiley-VCH Verlag GmbH, **2003**, pp. 145–192.

- [22] Y. Zhou, F. Ouyang, Z.-B. Song, Z. Yang, D.-J. Tao, *Catal. Commun.* **2015**, *66*, 25–29.
- [23] S. E. Kondawar, C. R. Patil, C. V. Rode, *ACS Sustain. Chem. Eng.* **2017**, *5*, 1763–1774.
- [24] D. Wilms, S.-E. Stiriba, H. Frey, *Acc. Chem. Res.* **2010**, *43*, 129–141.
- [25] A. Leal-Duaso, M. Caballero, A. Urriolabeitia, J. A. Mayoral, J. I. García, E. Pires, *Green Chem.* **2017**, *19*, 4176–4185.
- [26] S. Tanaka, T. Nakashima, T. Maeda, M. Ratanasak, J. Hasegawa, Y. Kon, M. Tamura, K. Sato, *ACS Catal.* **2018**, *8*, 1097–1103.
- [27] F. B. Gebretsadik, J. Ruiz-Martinez, P. Salagre, Y. Cesteros, *Appl. Catal. Gen.* **2017**, *538*, 91–98.
- [28] K. Kitaori, Y. Furukawa, H. Yoshimoto, J. Otera, *Tetrahedron* **1999**, *55*, 14381–14390.
- [29] S. R. Sandler, F. R. Berg, *J. Polym. Sci. [AI]* **1966**, *4*, 1253–1259.
- [30] E. J. Vandenberg, *J. Polym. Sci. Polym. Chem. Ed.* **1985**, *23*, 915–949.
- [31] Y. H. Kim, O. W. Webster, *J. Am. Chem. Soc.* **1990**, *112*, 4592–4593.
- [32] J. M. J. Fréchet, C. J. Hawker, *React. Funct. Polym.* **1995**, *26*, 127–136.
- [33] H. Frey, R. Haag, *Rev. Mol. Biotechnol.* **2002**, *90*, 257–267.
- [34] “Mephenesin,”
<https://www.drugs.com/international/mephenesin.html>, **2018**.
- [35] “GuaiFENesin (Professional Patient Advice),”
<https://www.drugs.com/ppa/guafenesin.html>, **2018**.
- [36] F. Della Monica, A. Buonerba, A. Grassi, C. Capacchione, S. Milione, *ChemSusChem* **2016**, *9*, 3457–3464.
- [37] R. Auvergne, S. Caillol, G. David, B. Boutevin, J.-P. Pascault, *Chem. Rev.* **2014**, *114*, 1082–1115.
- [38] C. D. Magnusson, G. G. Haraldsson, *Chem. Phys. Lipids* **2011**, *164*, 315–340.
- [39] H. K. Mangold, *Angew. Chem.* **1979**, *91*, 550–560.
- [40] M. Sutter, E. D. Silva, N. Duguet, Y. Raoul, E. Métay, M. Lemaire, *Chem. Rev.* **2015**, *115*, 8609–8651.
- [41] F. Snyder, *Ether Lipids Chem. Biol.* **1972**, 273–295.
- [42] J. I. García, H. García-Marin, E. Pires, *Green Chem.* **2014**, *16*, 1007–1033.
- [43] B. Z. Ngwenya, D. M. Foster, *Proc. Soc. Exp. Biol. Med.* **1991**, *196*, 69–75.
- [44] H. S. Ved, E. Gustow, V. Mahadevan, R. A. Pieringer, *J. Biol. Chem.* **1984**, *259*, 8115–8121.
- [45] A.-L. Deniau, P. Mosset, F. Pédrone, R. Mitre, D. L. Bot, A. B. Legrand, A.-L. Deniau, P. Mosset, F. Pédrone, R. Mitre, et al., *Mar. Drugs* **2010**, *8*, 2175–2184.
- [46] A. Suzuki, T. Yamaguchi, K. Kawasaki, T. Hase, I. Tokimitsu, *J. Pharm. Pharmacol.* **2002**, *54*, 1601–1607.

- [47] J. Alexander, J. M. Brewer, *Vaccines*, **1999**, US5876721A.
- [48] J. D. Engel, M. D. Mollière, I. D. Szelenyi, *Verwendung des Wirkstoffs Azelastin und Glycerinethern zur Bekämpfung von Psoriasis-Erkrankungen*, **1994**, EP0533213B1.
- [49] W. D. Beilfus, K.-H. Diehl, H. D. Eggensperger, P. D. Oltmanns, *Desodorierende Wirkstoffe*, **1994**, DE4240674C1.
- [50] D. Cauwet, C. Dubief, *Composition cosmétique contenant au moins un agent tensioactif de type alkylpolyglycoside et/ou polyglycérolé et au moins un uréthannepolyéther*, **1996**, EP0555155B1.
- [51] W. Beilfuss, S. Wutsch, K. Weber, R. Gradtke, *Composition Based on Glycerol Ether/Polyol Mixtures*, **2008**, US20080255015A1.
- [52] “sensiva® SC 50 - Schuelke & Mayr GmbH - Products 2019 - in-cosmetics Global,” can be found under <http://www.in-cosmetics.com/en/Exhibitors/4817996/Schuelke-Mayr-GmbH/Products/1410768/sensiva-SC-50>, **2018**.
- [53] G. G. Davies, I. M. Heilbron, W. M. Owens, *J. Chem. Soc. Resumed* **1930**, 0, 2542–2546.
- [54] P. Krafft, P. Gilbeau, *Manufacture of Dichloropropanol*, **2008**, WO2009000773A1.
- [55] R. Barbe, J. Hasserodt, *Tetrahedron* **2007**, 63, 2199–2207.
- [56] S. Berkowitz, *Preparation of Alkyl Glyceryl Ether Alcohols*, Google Patents, **1981**.
- [57] A. Sunder, R. Hanselmann, H. Frey, R. Mülhaupt, *Macromolecules* **1999**, 32, 4240–4246.
- [58] R. A. Johnson, C. E. Burgos, E. G. Nidy, *Chem. Phys. Lipids* **1989**, 50, 119–126.
- [59] R. K. Erukulla, H.-S. Byun, D. C. Locke, R. Bittman, *J. Chem. Soc. Perkin I* **1995**, 2199.
- [60] R. A. Sheldon, *Chem Soc Rev* **2012**, 41, 1437–1451.
- [61] S. Pariente, N. Tanchoux, F. Fajula, *Green Chem.* **2009**, 11, 1256–1261.
- [62] Y. Gu, A. Azzouzi, Y. Pouilloux, F. Jérôme, J. Barrault, *Green Chem.* **2008**, 10, 164–167.
- [63] F. Liu, K. D. O. Vigier, M. Pera-Titus, Y. Pouilloux, J.-M. Clacens, F. Decampo, F. Jérôme, *Green Chem.* **2013**, 15, 901–909.
- [64] P. Gaudin, R. Jacquot, P. Marion, Y. Pouilloux, F. Jérôme, *ChemSusChem* **2011**, 4, 719–722.
- [65] P. Gaudin, R. Jacquot, P. Marion, Y. Pouilloux, F. Jérôme, *Catal. Sci. Technol.* **2011**, 1, 616.
- [66] Y. Nakagawa, M. Tamura, K. Tomishige, *J. Mater. Chem. A* **2014**, 2, 6688–6702.
- [67] Y. Wang, J. Zhou, X. Guo, *RSC Adv.* **2015**, 5, 74611–74628.
- [68] C. J. Sullivan, in *Ullmanns Encycl. Ind. Chem.*, Wiley-VCH Verlag GmbH & Co. KGaA, **2000**.
- [69] G. A. Kraus, *CLEAN - Soil Air Water* **2008**, 36, 648–651.

- [70] Z. Yuan, J. Wang, L. Wang, W. Xie, P. Chen, Z. Hou, X. Zheng, *Bioresour. Technol.* **2010**, *101*, 7088–7092.
- [71] A. Bienholz, F. Schwab, P. Claus, *Green Chem.* **2010**, *12*, 290–295.
- [72] Y.-S. Feng, C. Liu, Y.-M. Kang, X.-M. Zhou, L.-L. Liu, J. Deng, H.-J. Xu, Y. Fu, *Chem. Eng. J.* **2015**, *281*, 96–101.
- [73] C.-H. (Clayton) Zhou, J. N. Beltramini, Y.-X. Fan, G. Q. (Max) Lu, *Chem. Soc. Rev.* **2008**, *37*, 527–549.
- [74] Y. Nakagawa, K. Tomishige, *Catal. Sci. Technol.* **2011**, *1*, 179–190.
- [75] F. Mauriello, H. Ariga, M. G. Musolino, R. Pietropaolo, S. Takakusagi, K. Asakura, *Appl. Catal. B Environ.* **2015**, *166–167*, 121–131.
- [76] M. G. Musolino, L. A. Scarpino, F. Mauriello, R. Pietropaolo, *ChemSusChem* **2011**, *4*, 1143–1150.
- [77] M. A. Dasari, P.-P. Kiatsimkul, W. R. Sutterlin, G. J. Suppes, *Appl. Catal. Gen.* **2005**, *281*, 225–231.
- [78] R. Lin, H. Liu, J. Hao, K. Cheng, D. Liu, *Biotechnol. Lett.* **2005**, *27*, 1755–1759.
- [79] Y. Kadowaki, M. Kaneda, H. Uchida, *Catalyst for Producing Both End-Hydroxyl Group-Terminated Diols, Process for Producing the Catalyst, Process for Producing the Diols by Using the Catalyst, and Both End-Hydroxyl Group-Terminated Diols Obtained by the Process*, **2007**, US7230145 B2.
- [80] R. Cucciniello, C. Pironti, C. Capacchione, A. Proto, M. Di Serio, *Catal. Commun.* **2016**, *77*, 98–102.
- [81] F. B. Gebretsadik, J. Llorca, P. Salagre, Y. Cesteros, *ChemCatChem* **2017**, *9*, 3670–3680.
- [82] M. De Torres, G. Jiménez-osés, J. A. Mayoral, E. Pires, M. de los Santos, *Fuel* **2012**, *94*, 614–616.
- [83] E.-E. Oprescu, E. Stepan, R. E. Dragomir, A. Radu, P. Rosca, *Fuel Process. Technol.* **2013**, *110*, 214–217.
- [84] M. R. Nanda, Y. Zhang, Z. Yuan, W. Qin, H. S. Ghaziaskar, C. (Charles) Xu, *Renew. Sustain. Energy Rev.* **2016**, *56*, 1022–1031.
- [85] L. Li, T. I. Korányi, B. F. Sels, P. P. Pescarmona, *Green Chem.* **2012**, *14*, 1611–1619.
- [86] A. Procopio, R. Dalpozzo, A. De Nino, L. Maiuolo, M. Nardi, B. Russo, *Adv. Synth. Catal.* **2005**, *347*, 1447–1450.
- [87] N. Iranpoor, F. Kazemi, *Synth. Commun.* **1998**, *28*, 3189–3193.
- [88] N. Iranpoor, H. Adibi, *Bull. Chem. Soc. Jpn.* **2000**, *73*, 675–680.
- [89] V. O. Samoilov, M. O. Onishchenko, D. N. Ramazanov, A. L. Maximov, *ChemCatChem* **2017**, *9*, 2839–2849.

2 MATERIALS AND METHODS

2.1 Materials

The compounds used as catalysts BiCl_3 , FeCl_3 , FeCl_2 , ZnCl_2 , AlCl_3 , $\text{Bi}(\text{OTf})_3$, $\text{Fe}(\text{OTf})_3$, $\text{Fe}(\text{OTf})_2$, $\text{Zn}(\text{OTf})_2$, $\text{Al}(\text{OTf})_3$, triflic acid, Nafion NR 50, Amberlyst 15 (A15), activated charcoal (AC), silica 30–60 mesh, graphene oxide (GO), montmorillonite K10 (M-K10), were purchased from Sigma-Aldrich (St. Louis, MO, USA).

Palladium on carbon (Pd/C) catalyst with a palladium content of 10 wt % was purchased from Acros.

$\text{Ag}(\text{OTf})$, sodium hydroxide, sulfuric acid, chlorosulfonic acid, cetyltrimethylammonium bromide (CTAB), tetraethylorthosilicate (TEOS), sulfonated polystyrene, glycidol (96 %), (R)-(+)-glycidol, (S)-(-)-glycidol, 1,2-propanediol (99.5 %), 1,3-propanediol (98 %), acetone, ethanol, methanol, 1-propanol, 2-propanol, 1-butanol, *tert*-butanol, 2-methyl-1-propanol, 3-methyl-1-butanol, 1-pentanol, 1-octanol, 2-ethyl-1-hexanol, benzyl alcohol, 3-pentanone, 2-butanone, tetrahydrofuran (THF), dichloromethane, 3-methoxy-1,2-propanediol, 1,2- isopropylidene glycerol were purchased from Sigma-Aldrich (St. Louis, MO, USA).

All the solvents were distilled before reactions and the catalysts were not pre-treated before reactions.

All manipulations were performed under a dry nitrogen atmosphere using a standard Schlenk techniques or Braun single station drybox.

Glycidol (96 %) was dried with CaH_2 or molecular sieves and distilled under reduced pressure before all experiments. The alcohols used were appropriately dried and purified by distillation under inert atmosphere.

All other chemicals were commercially available and used as received unless otherwise stated.

2.2 Catalysts synthesis

2.2.1 Synthesis of metal triflate supported catalysts

Triflates of Al(III), Bi(III), and Fe(III) supported on mesoporous silica (MPS) (named as Al(OTf)₃-MPS, Fe(OTf)₃-MPS and Bi(OTf)₃-MPS) were synthesized by using the following procedure.

First, the mesoporous silica was synthesized through basic hydrolysis of tetraethyl orthosilicate in the presence of cetyltrimethylammonium bromide as templating agent.

Sodium hydroxide (1.22 g) was added to a solution of cetyltrimethylammonium bromide (7.44 g) in distilled water (170 mL). Then, tetraethyl orthosilicate (17.68 g) was added dropwise to the resulting solution under vigorous stirring to give a gel that was left to stir at room temperature for 36 h. The mixture was then filtered, and the recovered solid was washed with distilled water and dried at 80 °C for 8 h. Finally, it was calcinated at 550 °C for 6 h in static air to get 4.45 g of mesoporous silica.

To obtain metal triflates supported on mesoporous silica, 1 g of the support was added to a 33 mM solution of metal triflate in toluene (25 mL) under nitrogen atmosphere. The resulting mixture is kept under magnetic stirring (300 rpm) at room temperature for 24 h. The mixture was then filtered and the solid was washed with toluene and dried at 100 °C in static air for 8 h.

2.2.2 Synthesis of sulfonated catalysts

Two methodology reported in literature (named as A or B) was employed for the synthesis of sulfonated mesoporous silica (MPS-SO₃H) and sulfonated silica (naked silica-SO₃H).

In the first one (A), silica (1g) was added to a 0.1 M solution of sulfuric acid (100 mL), keeping the mixture under stirring at room temperature for 24 h.^[90]

In the second one (B), chlorosulfonic acid (2.33 g) was added dropwise to silica (6.0 g) at room temperature in a mortar.^[91]

Sulfonated activated charcoal (AC-SO₃H) was synthesized using the methodology A as follow: to a 0.1 M solution of sulfuric acid (100 mL) was added 1 g of activated charcoal and the resulting mixture was kept under magnetic stirring at room temperature for 24 h.

2.2.3 Synthesis of [OSSO]-Iron(III) triflate complex

[OSSO]-Iron(III) triflate complex was prepared from the chloride analogous through substitution of the chloride ion with the triflate one using AgOTf as triflate ions source.

The synthesis of [OSSO]-Iron(III) chloride complex was performed as reported by Capacchione et al..^[92]

A solution of the ligand (2.069 g; 3.72 mmol) in 100 mL of THF was added to a suspension of sodium hydride (0.200 g; 8.30 mmol) in THF (45 mL). The mixture was stirred at room temperature overnight, after that it was filtered through celite. Then, it was slowly added to 0.591 g of anhydrous iron(III) chloride (3.64 mmol) dissolved in 100 mL of THF and the reaction kept overnight. A deep purple crystalline solid was recovered by filtration through celite and removal of the solvent under reduced pressure (yield: 2.406 g, 90.1 %).

A solution of the chlorine complex (2.055 g, 2.86 mmol) in CH₂Cl₂ (40 mL) was added to a solution of AgOTf (0.735 g, 2.86 mmol) in CH₂Cl₂ (40 mL) allowing it to stir at room temperature overnight. Then, the mixture was filtered through celite and the solvent was removed under reduced pressure.

The [OSSO]-Iron(III) triflate complex was obtained as deep purple crystalline solid (yield: 1.77 g, 74.5 %).

2.3 Catalysts characterization

2.3.1 Total acidity and BET surface area of heterogeneous acid catalysts

The Brønsted acidity of the heterogeneous catalysts (total acidity) were determined by titration with potassium hydroxide (0.03 M solution) using phenolphthalein as indicator.

The BET surface areas of the heterogeneous catalysts were measured using a Nova Quantachrome 4200e instrument determined with nitrogen as the probe molecule at liquid nitrogen temperature. Prior to the measurement, samples were degassed under vacuum for 12 h at 50 °C.

For the data extrapolation was used a 11-point BET analysis.

2.3.2 Metal content and infrared spectra of triflates supported catalysts

The metal amount (Al, Bi, Fe) for metal triflates supported on mesoporous silica was estimated by inductively coupled plasma optical emission spectroscopy (ICP-OES) using a PerkinElmer Optima 7000 DV (Wellesley, MA, USA) instrument.

The sample (78 mg for Al(OTf)₃-MPS, 38 mg for Fe(OTf)₃-MPS, 11 mg for Bi(OTf)₃-MPS) was dissolved in hydrofluoric acid (500 µL of a 40 % solution) and then made up to a volume of 25 mL in a volumetric flask with a 5 wt % boric acid solution. The resulting solution was diluted 100 times prior to be analysed.

Infrared spectra on metal triflates-based catalysts after pyridine adsorption were collected with Bruker spectrometers (Vertex70) equipped with deuterated triglycinesulphate (DTGS) detector and a KBr beam splitter in the range of 400-4000 cm⁻¹ with a resolution of 2 cm⁻¹.

For the measurement, 0.1 g of catalyst were treated at 120 °C for 2 h, then cooled in desiccator under vacuum and exposed to pyridine (25 mL) vapor for 12 h. The sample was then degassed under vacuum for 15 minutes to remove the physically adsorbed pyridine prior to be analysed.

2.3.3 X-ray diffraction and photoelectron spectroscopy of Pd/C-A15 system

X-ray diffraction (XRD) measurements were conducted on a Bruker D8 Advance automatic diffractometer operating with a nickel-filtered CuK α radiation, recording the data in the 2θ range of 4-80° with the resolution of 0.02°.

X-ray photoelectron spectroscopy (XPS) analyses were carried out by using a Kratos Axis Ultra electron spectrometer Al K α source (1486.6 eV) operated at 150 W (10 mA, 15 kV), recording the survey scan spectra with a pass energy of 160 eV and a 1 eV energy step. Using a pass energy of 20 eV and a 0.1 eV energy step, narrow scans were acquired. For all measurements was used a hybrid lens mode, an area about 700 x 300 μ m and a base pressure in the analysis chamber of 4.8×10^{-9} torr. During the acquisition of spectra, a system of charge compensation was used.

CasaXPS Release 2.3.16 software was used to process the spectra, the relative sensitivity factors listed in the library of the software for the areas of the signals were used for quantitative analysis were used.

The C1s graphitic component (284.4 eV) was used as reference for the binding energy (BE) scale.

2.3.4 Transmission electron microscopy of Pd/C-A15 system

Transmission electron microscopy (TEM) images were acquired using a TECNAI 20 G2: FEI COMPANY (CRYO-TEM-TOMOGRAPHY, Eindhoven) with a camera Eagle 2HS. For the analysis, the sample (10 μ L of a solution 1 mg/mL in DIW) was spread on a copper grid (200 mesh

with carbon membrane). The excess solution was removed, and the grids were dried overnight at room temperature. The images were acquired at 200 kV using a camera exposure time of 1 s with a size of 2048×2048 . A software-assisted approach using ImageJ (a cross-platform image analysis tool originated by the US NIH) was employed to estimate the particle size.

2.3.5 Morphological and elemental analysis of Pd/C-A15 system

Scanning electron microscope (SEM) images have been recorded on a Tescan Vega LMU microscope using secondary electrons (SE) with an accelerating voltage of 20.00 kV.

The Energy dispersive X-ray (EDX) spectra were acquired with an accelerating voltage of 20.00 kV and with a WD of 15.0 mm on a Bruker Quantax 800 energy dispersive microanalysis of elements with a resolution of $MnK\alpha$ less than 123 eV (100.000 cps) and an atomic number higher than 4. Using a standardless ZAF quantification, the X-Ray intensities were converted in wt % of elements.

2.3.6 NMR of [OSSO]-Iron(III) triflate complex

^{19}F -NMR spectra of [OSSO]-Iron(III) triflate complex were collected on Bruker Avance 400 MHz spectrometer.

Solution of [OSSO]-Iron(III) triflate complex were prepared in CD_3OD (1.2 mg in 0.7 mL) and in CD_2Cl_2 (1.8 mg in 1.0 mL) in a dry box.

As triflate standard was used a solution of 6 mg of $Al(OTf)_3$ dissolved in 0.6 mL of CD_3OD .

2.4 Experimental procedures

2.4.1 Recovery of 2-chloro-1,3-propanediol from chlorination mixture

The reaction products of glycerol chlorination (mixture of monochlorohydrins and dichlorohydrins) obtained as described by Vitiello

et al.^[12] have been separated through vacuum distillation at different temperatures.

Firstly, the temperature of the system has been set to 70 °C, in order to remove dichlorohydrins, then moved to 100 °C for the distillation of 3-chloro-1,2-propanediol, and 120 °C for that of 2-chloro-1,3-propanediol. The three distillation fractions were analysed by GC-FID.

2.4.2 Glycidol synthesis from monochlorohydrins

The synthesis of glycidol was performed using as starting material both monochlorohydrins mixture and 2-monochlorohydrin itself using the following procedure. In a 1 L round bottom flask, a solution of 0.1 moles of monochlorohydrin in distilled ethanol (20 mL) was added to a solution of 0.1 moles of potassium hydroxide in distilled ethanol (40 mL) under magnetic stirring (300 rpm).

The reaction was carried out for 30 minutes at room temperature after which it was filtered. Ethanol was distilled off in vacuum and the product was analysed by GC-FID.

2.4.3 Glycerol ethers synthesis

The first reactions are performed by using commercial homogeneous catalyst as follow. Glycidol (15 mmol) was added to a solution of the homogeneous catalysts (0.15-0.015 mmol) in alcohol (135 mmol) in a round bottom flask under N₂ atmosphere and the reaction mixture was heated at 80 °C for a fixed time under magnetic stirring (300 rpm). Afterwards, homogenous catalyst was removed by filtration on a plug of silica gel and the reaction products were analysed by GC-FID.

For the synthetic homogeneous catalyst, the procedure was modified as fallow. In a drybox, glycidol (1.5-3 mmol) was added to a solution of [OSSO]-Iron(III) triflate complex (0.0075-0.03 mmol) in alcohol (13.5-27

mmol), then the reaction mixture was heated at 80 °C for a fixed time under magnetic stirring (300 rpm). Subsequently, homogenous catalyst was removed by filtration on a plug of silica gel in a Pasteur pipet and the reaction products were analysed by GC-FID.

For heterogeneous catalysis, glycidol (15 mmol) and alcohol (135 mmol) were mixed together in a round-bottom flask under N₂ atmosphere, then the catalyst (0.05-0.2 g) was added and the reaction mixture was heated at 80 °C for a fixed time under magnetic stirring (300 rpm). Then, heterogenous catalyst was removed by filtration and the reaction products were analysed by GC-FID.

2.4.4 Propanediols synthesis

Hydrogenation reactions were performed in a pressure reactor with a capacity of 150 mL equipped with a glass vial containing a magnetic stirrer, 5 mL of distilled solvent, 1 mL of purified glycidol and 0.1 g of 10 % Pd/C in order to have a glycidol/Pd weight ratio of 100. After, an appropriate amount of A15 was added to the reaction mixture to have a A15 amount in the range 0.1–10 wt %. Experiments were carried out at 80 °C under a constant hydrogen pressure of 8 bars. Catalyst was removed by filtration and the reaction products were purified on celite before GC-FID analysis.

2.4.5 Glycerol ketals synthesis

Glycidol (350 µL) and of ketone (15.0-21 mL) were mixed together in a round bottom flask under magnetic stirring (300 rpm) for 24 h in reflux conditions in the presence of an appropriate amount of heterogeneous catalyst (glycidol/catalyst weight ratio of 10). Afterwards, heterogenous catalyst was removed by filtration, ketone was removed using a rotary evaporator and the reaction products were analysed by GC-FID.

2.5 Compounds analysis and quantification

The compounds of interest were analysed and quantified by using a gas chromatograph (GC) Thermo Trace equipped with a 30 m (0.32 mm i.d.) Fawax (polyethylene glycol as stationary phase) polar column and a flame ionization detector (FID).

Gas chromatography analyses were carried out by diluting an appropriate volume of the product sample to a final volume of 10 mL using ethanol in a volumetric flask.

The initial oven temperature was 40 °C, then it was programmed to heat to 160 °C at 5 °C min⁻¹, then to 230 °C at 20 °C min⁻¹, and held at 230 °C for 5 min with a flow rate of 1.0 mL min⁻¹. A splitless injection mode was used with an injection volume of 1 µL. The temperature was 280 °C for the detector and 230 °C for the inlet.

Each compound was calibrated in an appropriate range of concentrations, using an internal standard (1,2-isopropylidenglycerol or 3-ethoxy-1,2-propanediol). The integrated areas were converted into mole percentages for each component present in the sample by using the calibration curves.

High performance liquid chromatography (HPLC) analyses were performed by using cellulose tris-(3-chloro-4-methylphenylcarbamate) as chiral stationary phase and a mixture of *n*-hexane/2-propanol 77/23 v/v % as eluent with a flow rate of 0.4 mL min⁻¹. Samples were prepared by dissolving 0.200 mL of the product (purified by column chromatography) to a final volume of 10 mL with the eluent used for the analyses.

NMR spectra (¹H, ¹³C and ¹⁹F) were collected on Bruker Avance-400 spectrometer [400(¹H), 100(¹³C) and 376(¹⁹F)].

Magic angle spinning (MAS) solid state ¹³C-NMR spectra were recorded on a Bruker Avance-300 spectrometer [300(¹H) e 75.48(¹³C)] using a rotation speed of 11500 Hz and D₁ of 5 s. Adamantane was used as external ¹³C standard (peak at 29.5 ppm) for the calibration.

2.6 Life cycle assessment (LCA) methodology

The assessment of the environmental performances was carried out by Dr. Daniele Cespi and Prof. Fabrizio Passarini following a life cycle perspective.^[93]

Life cycle assessment (LCA) is a standardized methodology, whose general guidelines and framework are provided by ISO 14040 series^[94,95], which involves assessment of the environmental performances of a product or system within the more relevant stages of their life cycle.

Moreover, the cradle-to-gate approach was applied, that is an assessment of a partial product life cycle from resource extraction (cradle) to the factory gate (i.e., before it is transported to the consumer) omitting the use phase and disposal phase of the product. In this case, the production of the same amount (1 kg) of valuable products on the laboratory scale was considered as a functional unit (FU) to refer each input and output of the system under investigation.

The cradle-to-gate analysis was performed by using a licensed LCA software (SimaPro, version 8.0.4.30)^[96] and Ecoinvent database^[97]. Environmental scores such as carbon footprint (CF) and water footprint (WF) were used to investigate sustainability within the bio-based industry.^[93] On the other hand, the cumulative energy demand (CED, version 1.09)^[98] was chosen as indicator for the consumption of both renewable and non-renewable resources and the ReCiPe single-score (SS) (midpoint and endpoint level, version 1.11)^[99] was adopted to evaluate the global score reached by each scenario thanks to its property of covering different impact categories (climate change, land occupation and transformation, eutrophication and acidification) and of collecting them into a cumulative single score.

2.7 Density functional theory (DFT) calculations

The density functional theory (DFT) calculations were performed by Dr. Laura Falivene at the GGA BP86 level^[100-102] with the Gaussian09 package^[103]. The SVP basis set^[104] was used to describe the electronic configuration of all the systems. The M06 functional and the TZVP basis set^[105] were employed to build the reported free energies through single point energy calculations on the BP86/SVP geometries. The effects of the solvent (acetone) were included with the PCM model^[106,107]. Moreover, thermal corrections were added to this M06/TZVP electronic energy in solvent from the gas-phase frequency calculations at the BP86/SVP geometries. The catalyst structure has been modeled as in Chart 1 in order to streamline the calculations.

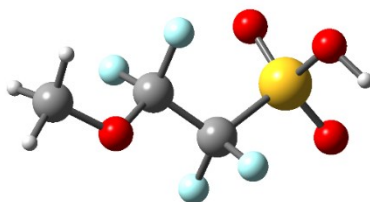


Chart 1. Catalyst structure modeled.

The chain end has been completely considered as $-\text{O}-\text{CF}_2-\text{CF}_2-\text{SO}_3\text{H}$, while the polymeric chain has been modeled as a $-\text{CH}_3$ group.

2.8 References

- [90] A. Karam, Y. Gu, F. Jérôme, J.-P. Douliez, J. Barrault, *Chem. Commun.* **2007**, 0, 2222–2224.
- [91] H. R. Shaterian, M. Ghashang, M. Feyzi, *Appl. Catal. Gen.* **2008**, 345, 128–133.
- [92] F. Della Monica, B. Maity, T. Pehl, A. Buonerba, A. De Nisi, M. Monari, A. Grassi, B. Rieger, L. Cavallo, C. Capacchione, *ACS Catal.* **2018**, 8, 6882–6893.
- [93] D. Cespi, F. Passarini, I. Vassura, F. Cavani, *Green Chem.* **2016**, 18, 1625–1638.
- [94] Environmental Management, Assessment of the Life Cycle, Principles and Framework; The International Organization for Standardization (ISO) 14040:2006 (en); Italian National Unification (UNI): Geneva, Switzerland, **2006**.
- [95] Environmental Management, Assessment of the Life Cycle, Requirements and Guidelines; The International Organization for Standardization (ISO) 14044:2006 (en); Italian National Unification (UNI): Geneva, Switzerland, **2006**.
- [96] PR8 Consultants, SimaPro, PhD version 8.3, Amersfoort, The Netherlands, **2016**, <https://www.pre-sustainability.com>.
- [97] Formerly Swiss Centre for Life Cycle Inventories; Ecoinvent Database 3.1; Ecoinvent Centre: Zurich, Switzerland, **2015**.
- [98] R. Frischknecht, N. Jungbluth, H.-J. Althaus, C. Bauer, G. Doka, R. Dones, R. Hirschler, S. Hellweg, S. Humbert, T. Köllner, Y. Loerincik, M. Margni and T. Nemecek, Implementation of Life Cycle Impact Assessment Methods, ecoinvent report No. 3, v2.0, Swiss Centre for Life Cycle Inventories, Dübendorf, **2007**.
- [99] M. Goedkoop, R. Heijungs, M. Huijbregts, A. de Schryver, J. Struijs, R. van Zelm, ReCiPe 2008—A Life Cycle Impact Assessment Method Which Comprises Harmonised Category Indicators at the Midpoint and the Endpoint Level, 1st ed. Version 1.08; Ministry of Housing, Spatial Planning and the Environment (VROM): The Hague, The Netherlands, **2013**.
- [100] A. D. Becke, *Phys. Rev. A* **1988**, 38, 3098–3100.
- [101] J. P. Perdew, *Phys. Rev. B* **1986**, 33, 8822–8824.
- [102] J. P. Perdew, *Phys. Rev. B* **1986**, 34, 7406–7406.
- [103] Frisch, M. J.; Trucks, G. W.; Schlegel, H. B.; Scuseria, G. E.; Robb, M. A.; Cheeseman, J. R.; Scalmani, G.; Barone, V.; Mennucci, B.; Petersson, G. A.; Nakatsuji, H.; Caricato, M.; Li, X.; Hratchian, H. P.; Izmaylov, A. F.; Bloino, J.; Zheng, G.; Sonnenberg, J. L.; Hada, M.; Ehara, M.; Toyota, K.; Fukuda, R.; Hasegawa, J.; Ishida, M.; Nakajima, T.; Honda, Y.; Kitao, O.; Nakai, H.; Vreven, T.; Montgomery, J. A.; Peralta, J. E.; Ogliaro, F.; Bearpark, M.; Heyd, J. J.; Brothers, E.; Kudin, K. N.; Staroverov, V. N.; Kobayashi, R.;

Normand, J.; Raghavachari, K.; Rendell, A.; Burant, J. C.; Iyengar, S. S.; Tomasi, J.; Cossi, M.; Rega, N.; Millam, J. M.; Klene, M.; Knox, J. E.; Cross, J. B.; Bakken, V.; Adamo, C.; Jaramillo, J.; Gomperts, R.; Stratmann, R. E.; Yazyev, O.; Austin, A. J.; Cammi, R.; Pomelli, C.; Ochterski, J. W. R.; Martin, L.; Morokuma, K.; Zakrzewski, V. G.; Voth, G. A.; Salvador, P.; Dannenberg, J. J.; Dapprich, S.; Daniels, A. D.; Farkas, Ö.; Foresman, J. B.; Ortiz, J. V.; Cioslowski, J.; Fox D. J. Gaussian 09 Revision A.1, Gaussian, Inc., Wallingford, CT, **2009**.

[104] A. Schäfer, H. Horn, R. Ahlrichs, *J. Chem. Phys.* **1992**, *97*, 2571–2577.

[105] A. Schäfer, C. Huber, R. Ahlrichs, *J. Chem. Phys.* **1994**, *100*, 5829–5835.

[106] J. Tomasi, M. Persico, *Chem. Rev.* **1994**, *94*, 2027–2094.

[107] V. Barone, M. Cossi, *J. Phys. Chem. A* **1998**, *102*, 1995–2001.

3 RESULTS AND DISCUSSION

3.1 Glycidol production form Epicerol® waste

Under the reported experimental conditions of glycerol chlorination^[12], a mixture of 1,3-dichloro-2-propanol (89.5 % in moles), 3-chloro-1,2-propanediol (0.6 % in moles), 1,2-dichloropropanol (2.4 % in moles) and 2-chloro-1,3-propanediol (7.5 % in moles as the main by-product) was formed after 4 h of reaction at 100 °C.

This chlorohydrins mixture was fractionated by vacuum distillation (Figure 26) in order to achieve pure 2-chloro-1,3-propanediol useful as glycidol precursor.

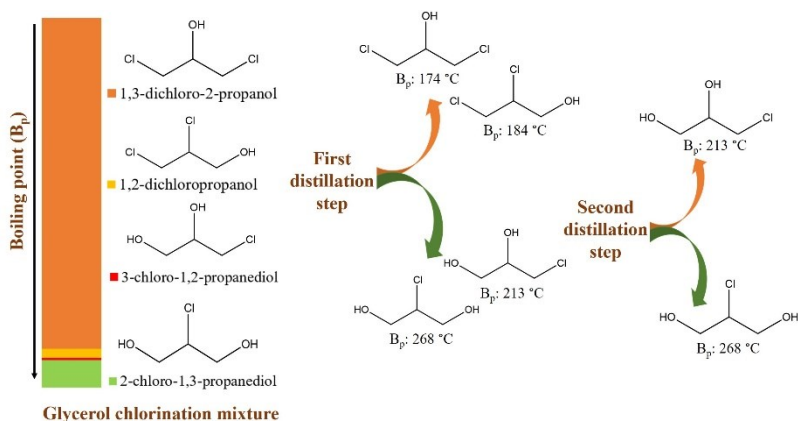


Figure 26. Schematic representation of the distillation of glycerol chlorination mixture: the bar with different colour indicates the mixture composition (%) and distribution in function of chlorohydrins boiling points.

Firstly, dichlorohydrins (1,3-dichloro-2-propanol and 1,2-dichloropropanol) were removed due to their lower boiling point (respectively 174 °C and 184 °C) compared to that of monochlorohydrins (213 °C for 3-chloro-1,2-propanediol and 268 °C for 2-chloro-1,3-propanediol).

An additional distillation step is required to separate 3-chloro-1,2-propanediol from 2-chloro-1,3-propanediol.

2-monochlorohydrin (2-chloro-1,3-propanediol) was converted with high yield (> 99 %) to glycidol in only 30 minutes at room temperature in an ethanolic solution of potassium hydroxide.

Moreover, the monochlorohydrins mixture was also tested in the production of glycidol, under the same reaction conditions adopted for 2-monochlorohydrin, giving the same yield in glycidol of the reaction performed with 2-monochlorohydrin alone (Figure 27) clearly showing that the last distillation step (the separation of 1-monochlorohydrin from 2-monochlorohydrin) could be avoided.

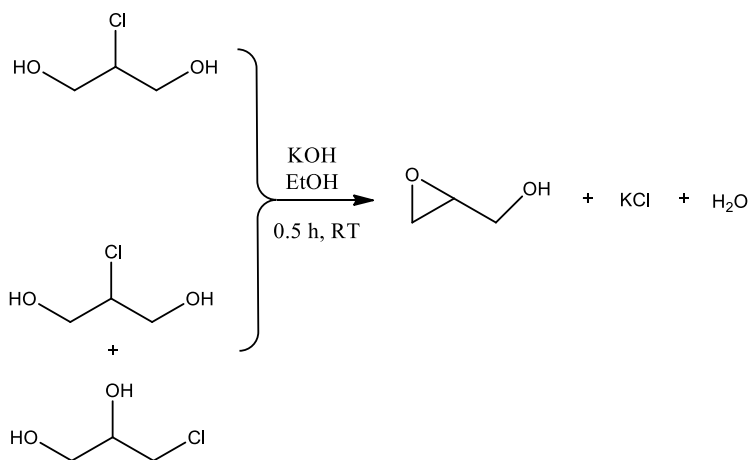


Figure 27. Synthesis of glycidol from monochlorohydrins.

Only potassium chloride and water were formed as by-products after the reaction and ethanol can be recovered by using a rotary evaporator and then reused.

In conclusion, an innovative methodology to recover 2-chloro-1,3-propanediol, the main by-product of the bio-based production of epichlorohydrin, from the mixture of glycerol chlorination has been proposed.

Moreover, this waste was efficiently used to produce glycidol (2,3-epoxy-1-propanol) through chlorine elimination and oxiranic function formation promoted by the basic action of potassium hydroxide.

The new synthetic pathway to synthesize glycidol was compared with the consolidated fossil-based route^[19] from allyl alcohol by using an early-stage life cycle assessment (LCA) analysis performed in collaboration with the research group of Professor Fabrizio Passarini.

This analysis shows that the proposed process encloses the Green Chemistry principles (use of renewable raw materials, increase of the atom economy and waste minimization), valorises the Epicerol® process by using its by-product and finally offers a new, economical way to obtain glycidol.

In light of the previous results, the research of new application of glycidol and its conversion in value-added products becomes a more promising synthetic strategy.

3.2 General properties of the catalysts

Both commercial and synthetic compounds used as catalysts in the conversion of glycidol, have been characterized with several techniques.

3.2.1 Total acidity and BET surface area

Total acidity and BET surface area of the heterogeneous catalysts are reported in Table 1.

Table 1. BET surface area and total acidity of the heterogeneous catalysts.

Catalyst	S BET (m ² /g)	Acid sites concentration (mmol/g)
MPS	1249	0.06
MPS-SO ₃ H-(A)	1060	0.15
MPS-SO ₃ H-(B)	210	4.80
Naked silica	90	0.03
Naked silica -SO ₃ H-(B)	58	3.75
AC	1506	0.03
AC-SO ₃ H	930	0.18
Nafion NR 50 beads	/	0.80
Amberlyst 15	37	4.70
M-K10	250	0.21
GO	460	0.48
Al(OTf) ₃ -MPS	642	1.50
Bi(OTf) ₃ -MPS	903	1.02
Fe(OTf) ₃ -MPS	770	1.72
Pd/C-A15	626	/

The results show a reduction of the surface area of supported samples in comparison of the support. This fact is indicative of the loading in the internal surface (inside the pores) of support. Moreover, the catalytic system formed by Pd/C and A15 displays a BET surface area lower than that of pure Pd/C (671 m²/g) due to the addition of Amberlyst 15.

3.2.2 Metal content and type of surface acidity

Metal content (Al, Bi and Fe) on the synthesized triflates supported on mesoporous silica was determined by using inductively coupled plasma optical emission spectroscopy (ICP-OES).

Results of the measurements show that metal content are: 0.51 mmol/g of Al in Al(OTf)₃-MPS (24 wt % of Al(OTf)₃ on MPS), 0.62 mmol/g of Bi in Bi(OTf)₃-MPS (41 wt % of Bi(OTf)₃ on MPS) and 0.62 mmol/g of Fe in Fe(OTf)₃-MPS (31 wt % of Fe(OTf)₃ on MPS).

The infrared (FT-IR) analysis confirms the presence of metal triflates in the supported samples (Figures 28-31).

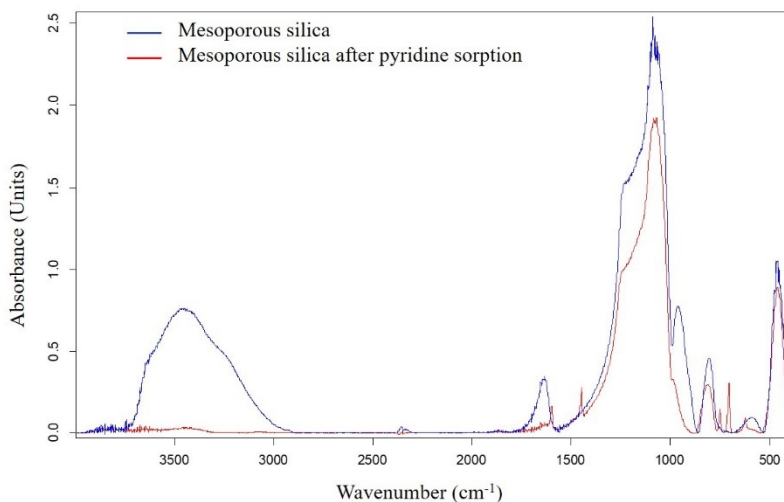


Figure 28. FT-IR spectra of mesoporous silica (blue line) and mesoporous silica after pyridine sorption (red line).

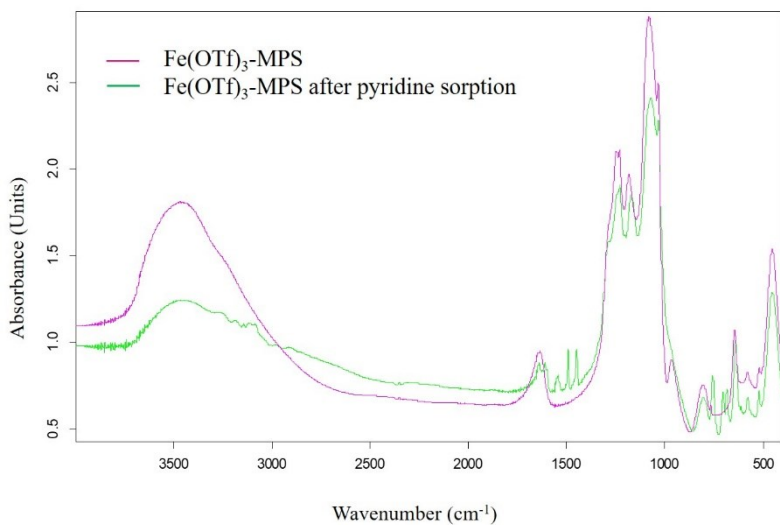


Figure 29. FT-IR spectra of Fe(OTf)₃ on mesoporous silica (pink line) and Fe(OTf)₃ on mesoporous silica after pyridine sorption (green line).

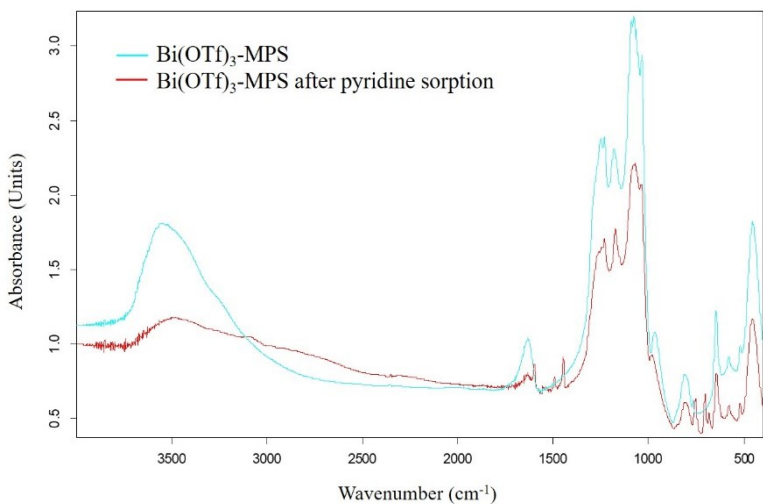


Figure 30. FT-IR spectra of Bi(OTf)₃ on mesoporous silica (light blue line) and Bi(OTf)₃ on mesoporous silica after pyridine sorption (red line).

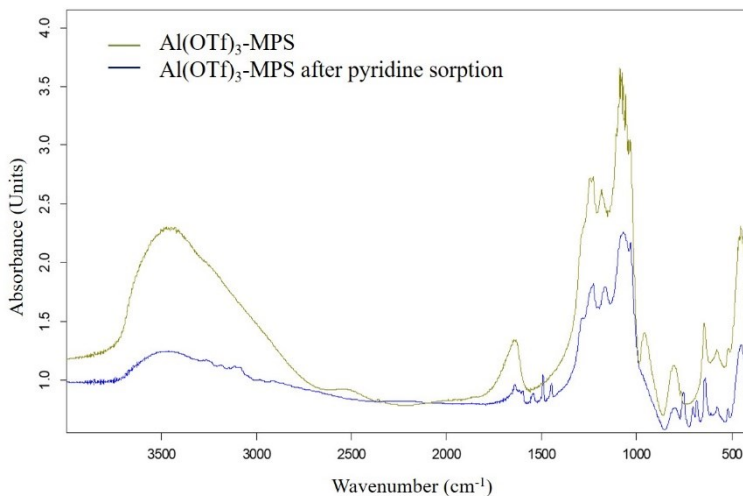


Figure 31. FT-IR spectra of $\text{Al}(\text{OTf})_3$ on mesoporous silica (dark green line) and $\text{Al}(\text{OTf})_3$ on mesoporous silica after pyridine sorption (blue line).

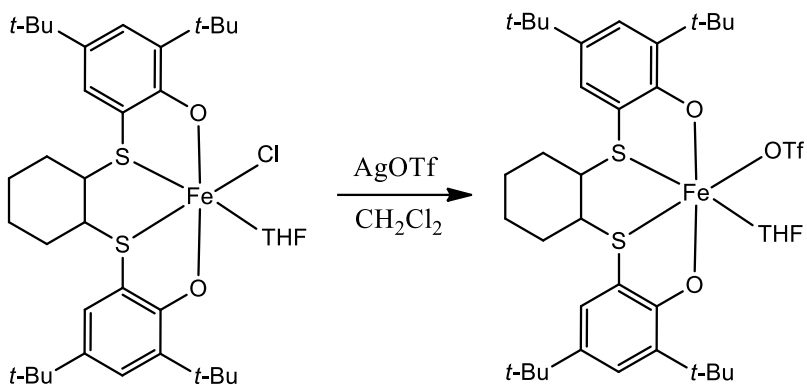
Analysing the spectra, a band at 1035 cm^{-1} was attributed to C-F stretching vibration of CF_3 - group while the bands in the range $1246\text{--}1185\text{ cm}^{-1}$ were attributed to S=O stretching and vibrations of SO_2 moieties.

FT-IR spectra recorded after pyridine adsorption were used to identify the type of surface acidity (Brønsted or Lewis).

The FT-IR studies of pyridine adsorbed samples (Figure 28-31) show the presence of both Lewis and Brønsted acidic sites in metal triflates-based catalysts as we can see from bands at 1446 cm^{-1} and 1543 cm^{-1} assigned to pyridine bound to Lewis and Brønsted acid sites, respectively and a band at 1494 cm^{-1} , representative of adsorbed pyridine at both the acidic sites.

3.2.3 [OSSO]-Iron(III) triflate complex

[OSSO]-Iron(III) triflate complex was synthesized from a precursor as reported in the experimental part (Scheme 1).



Scheme 1. Synthesis of [OSSO]-Iron(III) triflate complex .

¹⁹F-NMR spectra of the [OSSO]-Iron(III) triflate complex have been recorded in different solvents such as CD₂Cl₂ and CD₃OD (Figure 32).

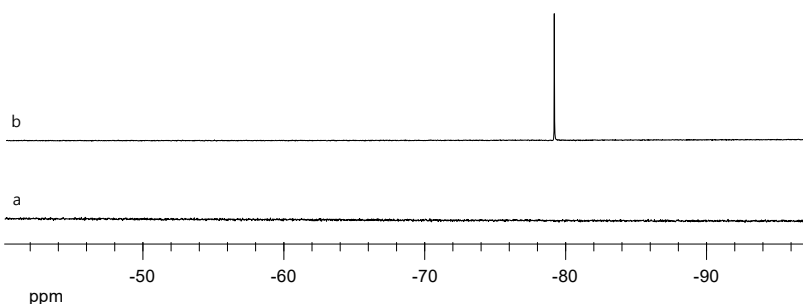


Figure 32. ¹⁹F-NMR (376 MHz) of [OSSO]-Iron(III) triflate complex in CD₂Cl₂ (a), and in CD₃OD (b).

As we can see from Figure 32 a, no signal is detected for the solution of the complex in CD_2Cl_2 , proving that the triflate ion is coordinated to Fe(III) in this solvent.

In CD_3OD , instead, a signal at -79 ppm appears in the ^{19}F -NMR spectrum (Figure 32 b). This is a typical signal of triflate ion^[108,109] as also showed in the ^{19}F -NMR spectrum of $\text{Al}(\text{OTf})_3$ (Figure 33).

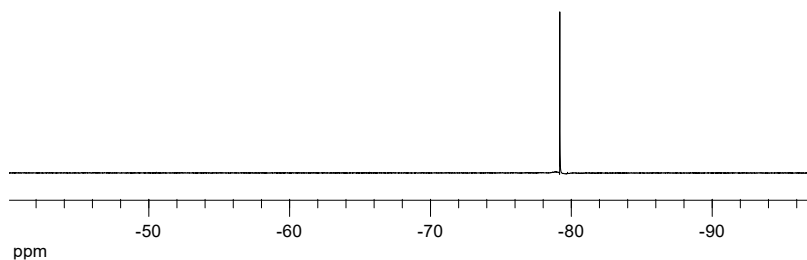
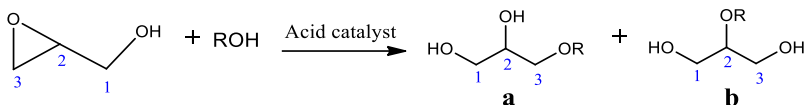


Figure 33. ^{19}F -NMR (376 MHz) of $\text{Al}(\text{OTf})_3$ in CD_3OD .

These results indicate that the methoxide ion replaces the triflate one in the coordination sphere of Fe(III) when the complex is dissolved in methanol.

3.3 Glycidol etherification with alcohols

For the first time, the ring opening reaction of glycidol with alcohols in the presence of an acid catalyst was investigated in the preparation of monoalkyl glyceryl ethers (Scheme 2).



Scheme 2. Catalytic ring-opening reaction of glycidol with alcohols.

Through this reaction, two regioisomeric products can be formed by the nucleophilic attack of the alcohol on the C2 or C3 carbon of glycidol.

Prior to explore the use of a catalyst, I have studied the un-catalysed ring opening reaction of glycidol using ethanol as benchmark in order to find the best reaction condition in terms of temperature and reactants composition avoiding the formation of by-products.

Therefore, in a first set of experiments, the reaction was investigated using an excess of ethanol in the range of temperatures 25-100 °C for 24 h.

In Figure 34 are reported conversions and selectivity of these reactions.

At 25 °C no etherification reaction takes place, whereas the increase of temperature has a moderate effect on the overall yield of the monoalkyl glyceryl ethers that grows from 5 % to 15 % in the conversion passing from 50 to 80 °C, maintaining a good selectivity toward monoalkyl glyceryl ethers (> 90 %). A further rise of the temperature leads to a conversion of 40 % with a concomitant severe loss of selectivity (70 % at 100 °C) due to the production of undesired glycidol oligomers.

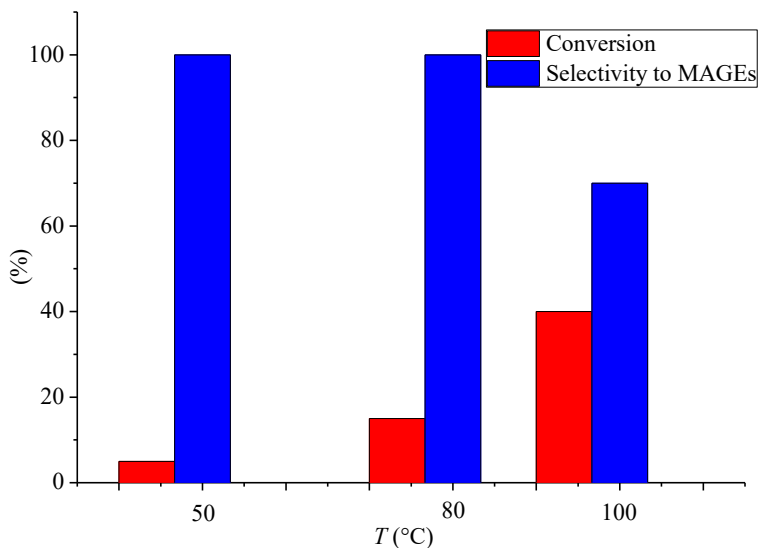


Figure 34. Effect of temperature on glycidol conversion and selectivity to MAGEs for uncatalyzed reactions using ethanol as nucleophile.

To optimize the glycidol/alcohol molar ratio, runs were performed at 80 °C varying the ethanol/glycidol molar ratio from 3 to 9. After 24 h of reaction, glycidol conversion is virtually the same at different ethanol/glycidol ratios but the selectivity to monoalkyl glyceryl ethers decreases by decreasing of ethanol/glycidol ratio due, again, to the glycidol oligomerization (91 % using ethanol/glycidol moles ratio 9, 81 % using ethanol/glycidol moles ratio of 5, 75 % using ethanol/glycidol moles ratio of 3).

Therefore, the temperature of 80 °C and the ethanol/glycidol molar ratio of 9 was chosen for the catalytic runs in order to hamper the formation of glycidol oligomers.

3.4 Etherification reactions catalysed by homogeneous catalysts

3.4.1. Catalytic screening of metal salts

This study was started testing homogeneous Lewis acid catalysts reported in literature as very active in the direct etherification of glycerol with alcohols.^[63]

A catalytic screening of different Lewis acid catalysts was performed at 80 °C, using the ethanol/glycidol molar ratio of 9 and the catalyst loading of 1 % in moles. The main results are summarized in Table 2.

Table 2. Glycidol etherification with ethanol in the presence of Lewis acids.

Entry	Catalyst	Conversion [%]	Selectivity to MAGEs [%]	a/b ratio [%]	TOF [h ⁻¹]
1	AlCl ₃	5	100	n.d.	5
2	BiCl ₃	22	100	n.d.	22
3	FeCl ₃	10	100	n.d.	10
4	FeCl ₂	1	100	n.d.	1
5	ZnCl ₂	1	100	n.d.	1
6	Al(OTf) ₃	100	92	80/20	1100*
7	Bi(OTf) ₃	100	89	75/25	1070*
8	Fe(OTf) ₃	100	91	75/25	1090*
9	Fe(OTf) ₂	62	100	>90/10	62
10	Zn(OTf) ₂	88	100	>90/10	88

Reaction conditions: 1.0 mL of glycidol, 8.0 mL of ethanol, 1 mol % of catalyst, 80 °C, 300 rpm, inert atmosphere, 1 h; *This value is based on the conversion at 5 minutes; n.d.: not detected; TOF: turnover frequency.

Among all the tested catalysts, the best results in terms of conversion and selectivity were obtained in the presence of metal triflates (Table 2, entry 6-10). In particular, triflates of metal in the oxidation state III such as Al(III), Fe(III) and Bi(III) show a higher catalytic activity compared to that of triflates of metal in the oxidation state II such as Fe(II) and Zn(II) that maintain a complete selectivity to the desired products.

The corresponding metal chlorides employed in this screening are instead less active in this transformation, probably due to the lower Lewis acidity compared to that of triflates.

Concerning the regioselectivity, the etherification reaction occurred with the preferential formation of terminal monoalkyl glyceryl ethers (regioisomer a) in all cases.

3.4.2 Metal triflates as catalysts

Further catalytic experiments have been performed with the most active Al(III), Fe(III) and Bi(III) triflates reducing the catalyst loading to 0.01 % in order to optimize the catalyst loading for this synthetic pathway (Table 3).

Table 3. Glycidol etherification with ethanol in the presence of metal triflates.

Entry	Catalyst	Conversion [%]	Selectivity to MAGEs [%]	TOF [h ⁻¹]
1	Al(OTf) ₃	100	93	13400*
2	Bi(OTf) ₃	100	99	9500*
3	Fe(OTf) ₃	92	91	8400
4	TfOH	81	88	7100

Reaction conditions: 1.0 mL of glycidol, 8.0 mL of ethanol, 0.01 mol % of catalyst, 80 °C, 300 rpm, inert atmosphere, 1h; *This value is based on the conversion at 30 minutes (72 % for Al(OTf)₃ and 48 % for Bi(OTf)₃); The a/b ratio is 75/25 for all the run; TOF: turnover frequency.

Delightfully, decreasing the catalyst loading, the quantitative conversion of glycidol to monoethoxy glyceryl ethers was achieved in only 1 h in the presence of both Bi(OTf)₃ and Al(OTf)₃ preserving high selectivity (93-99 %). On the contrary, Fe(OTf)₃ is less active than Bi(OTf)₃ and Al(OTf)₃ reaching lower conversion (92 %) and selectivity, under the same reaction conditions.

Finally, the etherification reaction was also performed using triflic acid (a Brønsted acid) as catalyst instead of metal triflate with a loading of 0.01 %

in moles. Monoalkyl glyceryl ethers were obtained with a lower conversion (81 %) and selectivity (88 %) compared to that attained in the presence of metal triflate. This aspect underlines the fundamental role of the Lewis acidic center in determining the catalytic activity and selectivity. Furthermore, the stability of the catalytic system based on $\text{Al}(\text{OTf})_3$, the most active metal triflate employed, was also explored.

For this scope, at the end of the reaction between glycidol and ethanol catalyzed by 0.01 % in moles of $\text{Al}(\text{OTf})_3$, an extra amount of glycidol was added to the reaction medium in order to restore the ethanol/glycidol molar ratio of 9. Then the mixture was left to further react, and it was analyzed again.

Noteworthy, the yield of monoethoxy glyceryl ethers remained constant after four consecutive additions showing that the catalyst was lasting under the investigated reaction conditions.

3.4.2.1 Different alcoholic substrates as nucleophiles

With the aim to extend the scope of the reaction, a wide range of alcoholic substrates were used as nucleophiles in the etherification reaction of glycidol in the presence of both $\text{Al}(\text{OTf})_3$, $\text{Bi}(\text{OTf})_3$ and $\text{Fe}(\text{OTf})_3$ at 80 °C with a catalyst loading of 0.01 % in moles (Table 4-6).

As one can see from the inspection of Table 4, $\text{Al}(\text{OTf})_3$ affords to give good conversion and selectivity for the etherification of glycidol with all the substrates tested, from short-chain alcohols to long-chain alcohols and benzyl alcohol, notwithstanding differences in term of polarity of the reaction media.

Indeed, a decrease in the catalytic activity was only observed by increasing the length of the alcoholic alkyl chain from butyl to octyl (conversion from 94 to 23 %).

Table 4. Catalytic etherification of glycidol with alcohols in presence of Al(OTf)₃.

Entry	-R	Conversion [%]	Selectivity to MAGEs [%]	a/b ratio [%]	TOF [h ⁻¹]
1	methyl	100	94	67/33	16000*
2	ethyl	100	93	75/25	13400*
3	<i>iso</i> -propyl	85	87	75/25	7400
4	<i>tert</i> -butyl	7	76	78/22	530
5	<i>n</i> -butyl	94	91	70/30	8500
6	<i>n</i> -pentyl	81	92	68/32	7400
7	<i>n</i> -octyl	23	51	70/30	1200
8	benzyl	99	99	60/40	9800

Reaction conditions: 1.0 mL of glycidol (15 mmol), 135 mmol of alcohol, 0.01 mol % of Al(OTf)₃, 80 °C, 300 rpm, inert atmosphere, 1 h; *This value is based on the conversion at 30 minutes (85 % for methanol and 72 % for ethanol); TOF: turnover frequency.

In the case of benzyl alcohol, the corresponding ether is produced with high activity (99 % of conversion and selectivity) while lower yield is achieved with *tert*-butanol probably due to the concomitant dehydration of the substrate.^[110]

Table 5. Glycidol etherification with alcohols in the presence of Bi(OTf)₃.

Entry	-R	Conversion [%]	Selectivity to MAGEs [%]	a/b ratio [%]	TOF [h ⁻¹]
1	methyl	100	95	70/30	17100*
2	ethyl	100	93	75/25	9500*
3	<i>iso</i> -propyl	86	84	75/25	7220
4	<i>tert</i> -butyl	8	98	83/17	780
5	<i>n</i> -butyl	95	91	75/25	8650
6	<i>n</i> -pentyl	28	84	75/25	2350
7	<i>n</i> -octyl	15	96	79/21	1440
8	benzyl	62	97	83/17	6010

Reaction conditions: 1.0 mL of glycidol (15 mmol), 135 mmol of alcohol, 0.01 mol % of Bi(OTf)₃, 80 °C, 300 rpm, inert atmosphere, 1 h; *This value is based on the conversion at 30 minutes (88 % for methanol and 48 % for ethanol); TOF: turnover frequency.

As in the case of $\text{Al}(\text{OTf})_3$, in the presence of 0.01 % mol of $\text{Bi}(\text{OTf})_3$ (Table 5) glycidol was quantitatively converted with high selectivity (> 93 %) into MAGEs using methanol and ethanol and a moderate decrease on conversion was observed by increasing the steric hindrance of the alcohol. Worse results than those obtained with $\text{Al}(\text{OTf})_3$ were achieved using pentanol and benzyl alcohol as nucleophiles.

Table 6. Catalytic etherification of glycidol with alcohols in presence of $\text{Fe}(\text{OTf})_3$.

Entry	-R	Conversion [%]	Selectivity to MAGEs [%]	a/b ratio [%]	TOF [h^{-1}]
1	methyl	93	96	70/30	8930
2	ethyl	92	91	75/25	8370
3	<i>iso</i> -propyl	88	68	78/22	5980
4	<i>tert</i> -butyl	32	99	88/12	3170
5	<i>n</i> -butyl	77	96	75/25	7390
6	<i>n</i> -pentyl	52	97	74/26	5040
7	<i>n</i> -octyl	37	98	75/25	3630
8	benzyl	51	99	71/29	5050

Reaction conditions: 1.0 mL of glycidol (15 mmol), 135 mmol of alcohol, 0.01 mol % of $\text{Fe}(\text{OTf})_3$, 80 °C, 300 rpm, inert atmosphere, 1 h. TOF: turnover frequency.

Results reported in Table 6 show that $\text{Fe}(\text{OTf})_3$ was less active than $\text{Al}(\text{OTf})_3$ and $\text{Bi}(\text{OTf})_3$ triflate, not giving total conversion of glycidol in the reaction with methanol and ethanol. Analogously, the same trend in the reduction of the catalytic activity with the increase of the length of the alcoholic alkyl chain was observed. Notably, better results were achieved in the etherification reaction using *tert*-butanol as nucleophile.

In addition, for the performed runs, carbon mass balance calculated on glycidol is always higher than 95 %, and the regioselectivity to terminal monoalkyl glyceryl ether (regioisomer a) is at least 60 %.

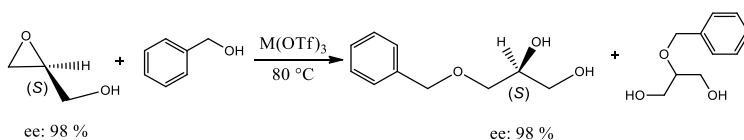
The poor regioselectivity observed is not a problem for applications such as solvent, additive and so on, because, in these cases, a mixture of regioisomers can be used thank to the similar physical-chemical properties of both products. Conversely, for specialty applications, such as biological and pharmaceutical, it is a great drawback because only one isomer must be used, and the separation of these compounds is usually difficult due to their chemical similarity if there are present in comparable amounts.

3.4.2.2 Enantiopure glycidol as starting material

In order to get deeper insights into the stereochemical factors governing the reaction, etherification reactions were also performed using the two enantiomerically pure glycidols, (*S*)-glycidol and (*R*)-glycidol.

Benzyl alcohol was used as alcoholic substrate for these reactions, that were carried out using both Al(OTf)₃ and Bi(OTf)₃ as catalysts under the optimized reaction conditions previously described (catalyst loading of 0.01 % mol, 80 °C).

As shown in Scheme 3, the chiral isomer 3-benzyloxy-1,2-propanediol, produced from the nucleophilic attack at C3 carbon of glycidol, have the same absolute configuration of the glycidol where we started from, so the reaction happens with the complete retention in configuration of the C2 carbon of glycidol.



Scheme 3. Etherification of enantiopure glycidol with benzyl alcohol (only (*S*)-glycidol is shown as example).

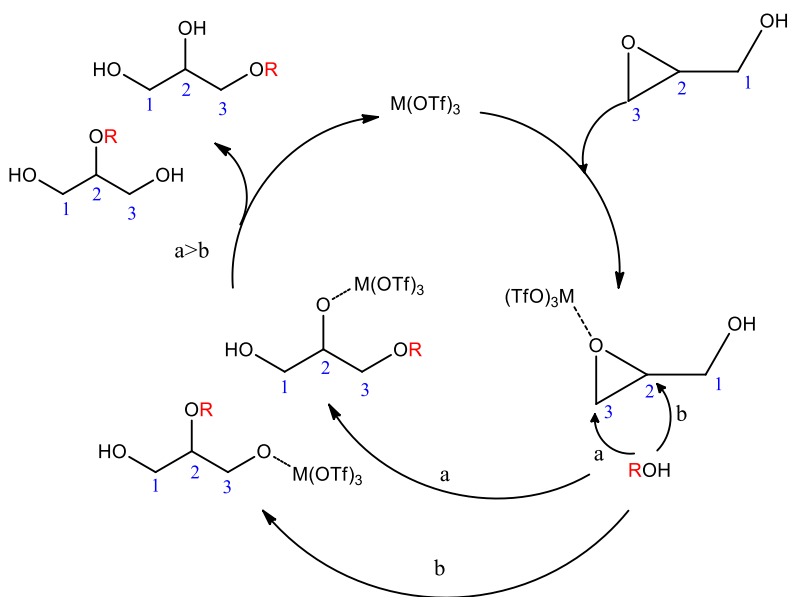
The nucleophilic attack at the more hindered C2 carbon of glycidol, instead, produces the achiral isomer (2-benzyloxy-1,3-propanediol).^[111]

These experiments, in addition to the useful information about the reaction mechanism, offer a new feasible route to chiral monobenzyl ethers that are important chiral building blocks for the synthesis of many biologically active compounds.^[112]

3.4.2.3 Plausible reaction mechanism

Based on the obtained catalytic results, a plausible reaction mechanism was proposed as reported in Scheme 4.

The oxiranic ring of glycidol is activated to the nucleophilic attack of the alcohol through the coordination of the epoxydic oxygen atom to the Lewis acidic metal center. Then the alcoholic addition can occur at the C3 carbon (less substituted) (a) or at the C2 carbon (more hindered) (b) of the epoxide ring.



Scheme 4. Plausible reaction mechanism.

Catalytic results show the preferential formation of terminal monoalkyl glyceryl ether (a isomer) resulting from nucleophilic attack of the alcohol on the less hindered carbon of glycidol.

Besides, the reduction of the conversion and the increasing of the a/b ratio with the increasing of the length and of the steric bulk of the alcoholic chain, together with the complete retention in configuration of the C2 carbon observed in the reaction performed with enantiopure glycidol, are fully in agreement with the hypothesized reaction mechanism.

3.4.2.4 Detailed study of monobutyl glycerol ether production

A detailed study of monobutyl glycerol ether synthesis was performed using Bi(OTf)₃ as catalyst in the etherification of glycidol with *n*-butanol. First of all, the aim of this investigation was to obtain experimental data that could be directly compared with the results reported in literature concerning the conversion of glycerol to monobutyl glycerol ether using Bi(OTf)₃ as homogeneous catalyst.^[63]

Furthermore, *n*-butanol has recently been recognized as a sustainable feedstock, as it can be obtained from bioethanol by its catalytic coupling.^[113]

Under the optimized reaction conditions previously described (80 °C, 0.01 % in moles of Bi(OTf)₃, alcohol/glycidol molar ratio of 9), glycidol conversion and selectivity to monobutyl glycerol ethers were detected at different reaction time as is shown in Figure 35.

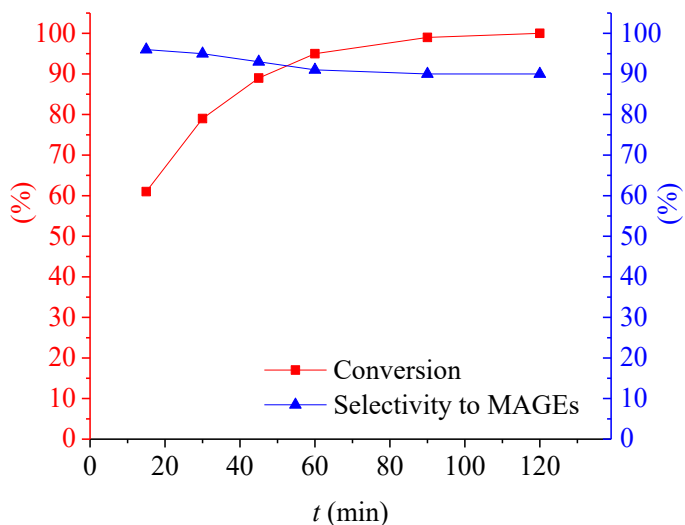


Figure 35. Glycidol etherification with *n*-butanol using Bi(OTf)₃ at 80 °C.

Total conversion of glycidol was reached in only 2 h with high selectivity (90 %) to monobutoxy glyceryl ether.

As we can see from Figure 36, the synthesis of monobutyl glycerol ethers from glycidol have some advantages in term of reaction conditions. Moreover, others significative benefits reside in the separation of the final products.

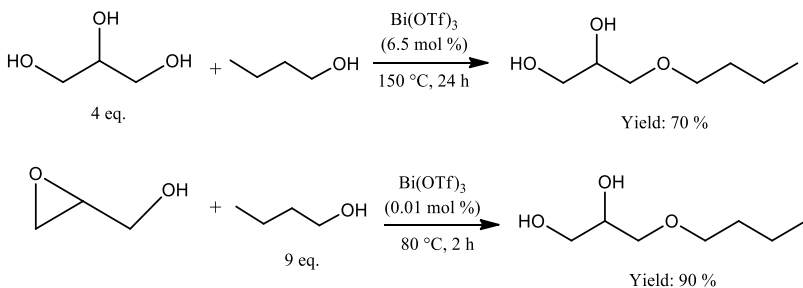


Figure 36. Comparison of monobutyl glycerol ether synthesis from glycerol and glycidol.

The proposed route, in fact, allows to gain pure butanoxyglyceryl ether (boiling point > 220 °C) removing the excess of *n*-butanol (boiling point of 118 °C) under vacuum distillation. On the contrary, the glycerol-based route has a major drawback arising from the use of an excess of glycerol (boiling point of 290 °C) that remains unreacted at the end of the reaction, and could react at high temperatures in the presence of the catalyst to form polyglycerols, resulting in a mixture from which the desired product cannot be easily recovered.^[114]

Actually, this is an important aspect to take into account for the implementation of a new synthetic strategy from the laboratory scale to the industrial level and it is related to the potential investments.^[115]

Finally, life cycle assessment (LCA) analyses were performed in collaboration with the research group of Professor Fabrizio Passarini using primary data obtained at the laboratory scale in order to compare the environmental sustainability of the proposed innovative synthetic route respect to using glycerol as starting material.

Results of this evaluation showed some potential advantages, suggesting that the use of glycidol as reagent and bismuth triflate as catalyst is a valuable alternative to reduce the environmental loads.

Moreover, the recovery of a byproduct from an industrial process (Epicerol® in this case) and its reutilization to synthesize high value products is a way to decrease the reliance on fossil-based sources.

3.4.3 [OSSO]-Iron(III) triflate complex as catalyst

Taking into account the previous results obtained with $\text{Fe}(\text{OTf})_3$, I tested the behavior of the [OSSO]-Iron(III) triflate complex (Figure 37) as catalyst for the etherification of glycidol in order to improve the selectivity towards the formation of terminal monoalkyl glyceryl ethers (regioisomer a).

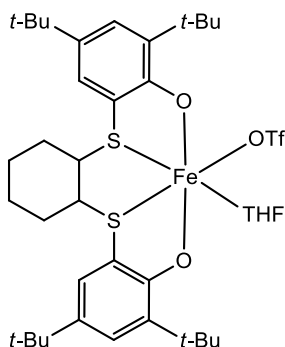


Figure 37. Structure of the [OSSO]-Iron(III) triflate complex.

In fact, for the production of glycerol monoethers suitable for application in biological and pharmaceutical fields, the regioselectivity of the reaction is a very important issue as previously mentioned.

3.4.3.1 Screening of the experimental conditions

Firstly, the reactions were performed at 80 °C, using ethanol as nucleophile (ethanol/glycidol molar ratio of 9) with a catalyst loading of 0.1 % in moles at different reaction time (Table 7).

Table 7. Glycidol etherification with ethanol in the presence of 0.1 mol % of [OSSO]-Iron(III) triflate complex.

Entry	Time [h]	Conversion [%]	Selectivity to MAGEs [%]	a/b ratio [%]	TOF [h ⁻¹]
1	1	63	96	90/10	600
2	2	88	95	90/10	418
3	3	91	94	90/10	287
4	4.5	99	95	90/10	-

Reaction conditions: 0.200 mL of glycidol (3 mmol), 27 mmol of ethanol, 0.1 mol % of catalyst, 300 rpm, inert atmosphere, 80 °C; TOF: turnover frequency.

Under these reaction conditions, total conversion of glycidol was achieved after 4.5 h with very high selectivity towards monoalkyl glyceryl ethers, and also a higher a/b ratio respect to that reached with Fe(OTf)₃ and the others metal triflates previously employed.

The effect of reaction temperature was also investigated performing the catalytic run in the range 30-80 °C using a catalyst loading of 0.1 % in moles (Table 8).

Table 8. Glycidol etherification with ethanol in the presence of the [OSSO]-Iron(III) triflate complex at different reaction temperature.

Entry	T[°C]	Conversion [%]	Selectivity to MAGEs [%]	a/b ratio [%]	TOF [h ⁻¹]
1	30	11	99	n.d.	22
2	40	23	99	86/14	64
3	50	36	99	85/15	86
4	60	72	97	88/12	157
5	70	87	96	89/11	186
6	80	99	95	90/10	-

Reaction conditions: 0.200 mL of glycidol (3 mmol), 27 mmol of ethanol, 0.1 mol % of catalyst, 300 rpm, inert atmosphere, 4,5 h; n.d.: not detected; TOF: turnover frequency.

A drastic decrease of glycidol conversion is observed at lower reaction temperature together with an increase of the selectivity to monoalkyl

glyceryl ethers, underlining the fact that the oligomerization of glycidol is reduced at lower temperature. However, the reduction of temperature does not give a significant improvement of the a/b ratio.

Therefore, the reaction temperature of 80 °C was, also in this case the best one for glycidol etherification reaction.

The influence of catalyst loading was also studied, performing the reaction with three amounts of catalyst as reported in Table 9.

Table 9. Glycidol etherification with ethanol in the presence of the [OSSO]-Iron(III) triflate complex at different catalyst loading.

Entry	Fe [mol %]	Gly/Fe molar ratio	Conversion [%]	Selectivity to MAGEs [%]	a/b ratio [%]	TOF [h ⁻¹]
1	0,1	1000	88	95	90/10	418
2	0,067	1500	80	95	89/11	570
3	0,05	2000	70	95	89/11	665

Reaction conditions: 0.200 mL of glycidol (3 mmol), 27 mmol of ethanol, 80 °C, 300 rpm, inert atmosphere, 2 h; TOF: turnover frequency.

Remarkably, even using a catalyst loading of 0.05 % in moles a good conversion and a high selectivity were achieved in only 2 h of reaction at 80 °C.

Moreover, the kinetic profile of the reaction (Figure 38) was investigated under these conditions using ethanol as nucleophile (ethanol/glycidol molar ratio of 9).

As one can see observe in Figure 38, the reaction reaches an initial turnover frequency of 1680 h⁻¹ (conversion of 28 % after 20 minutes), then after about 2 h the rate decrease, and the conversion increase very slowly until 88 % at 300 minutes since the start of the reaction.

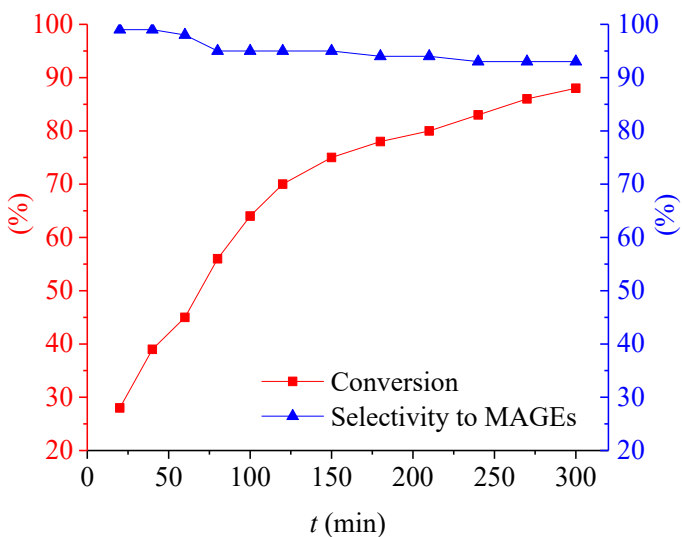


Figure 38. Kinetic profile of the etherification of glycidol catalysed by 0.05 % in moles of [OSSO]-Iron(III) triflate complex.

Very high selectivity to monoethoxy glyceryl ethers is attained at the start of the reaction (99 %), that in the end reach a plateau around a value of 94 %. The a/b ratio was virtually unchanged during the reaction ranging from 88/12 to 90/10.

3.4.3.2 Substrate scope extension

Finally, this catalytic system was used for the etherification of glycidol with a wide range of alcoholic substrates using a catalyst loading of 0.05 % in moles and a temperature of 80 °C (Table 10).

The [OSSO]-Iron(III) triflate complex is able to catalyse the reaction of glycidol with all the substrates tested without a significant variation of the activity changing the length of the alkyl chain, in contrast to the results obtained with $\text{Fe}(\text{OTf})_3$.

The lowest conversion at 80 °C was achieved by using methanol as nucleophile probably due to an instability of the complex in a methanolic solution at that temperature.

Nevertheless, methoxy glyceryl ethers were obtained with high selectivity performing the reaction at 40 °C with a catalyst loading of 0.5 % in moles.

Table 10. Glycidol etherification with different alcohols in the presence of the [OSSO]-Iron(III) triflate complex.

Entry	-R	Conversion [%]	Selectivity to MAGEs [%]	a/b ratio [%]	TOF [h ⁻¹]
1	methyl	8	99	n.d.	158
2*	methyl	99	94	90/10	8
3	ethyl	44	98	89/11	862
4	<i>n</i> -propyl	46	99	90/10	911
5	<i>iso</i> -propyl	60	96	93/7	1152
6	<i>n</i> -butyl	42	97	90/10	815
7	<i>iso</i> -butyl	57	96	90/10	1094
8	<i>tert</i> -butyl	40	97	96/4	776
9	<i>n</i> -pentyl	42	99	87/13	832
10	<i>iso</i> -pentyl	38	99	88/12	752
11	<i>iso</i> -octyl	41	99	91/9	812
12	<i>n</i> -octyl	38	99	88/12	752
13	benzyl	40	95	84/16	760

Reaction conditions: 0.100-0.200 mL of glycidol (1.5-3 mmol), 13.5-27 mmol of alcohol, 0.05 mol % of catalyst, 300 rpm, inert atmosphere, 80 °C, 1h; *40 °C, 0.5 mol % of catalyst, 24 h; n.d.: not detected; TOF: turnover frequency.

Very good results are attained with *iso*-propanol and *tert*-butanol despite the steric hindrance of their alkyl chain, reaching turnover frequency close to 1200 h⁻¹.

Concerning the regioselectivity, good a/b ratios were achieved for all the substrates tested, with the best result for the alcohols having a more hindered alkyl chain (Table 10, entry 5 and 8).

3.5 Heterogeneous catalysis for glycidol etherification

By considering the advantages of heterogeneous catalysis respect to the homogeneous one, the etherification reaction of glycidol was also investigated in the presence of heterogeneous acid catalysts.

In fact, the possibility to recover the expensive catalyst by separating it from the reaction mixture in a straightforward manner and use it for several times is an important consideration for industrial manufacturing processes.

3.5.1 Catalytic screening of commercial and synthetic acid catalysts

A systematic screening of several heterogeneous acid catalysts (both Lewis and Brønsted acids) was performed by using ethanol as nucleophile, a catalyst loading of 10 wt % and a temperature of 80 °C (Table 11).

Both Lewis and Brønsted heterogeneous acid catalysts gave the desired products under the investigated reaction conditions with results in line with their concentration of acid sites (see Table 1).

In all cases the etherification reaction proceeds with the preferential formation of terminal MAGEs (see a/b ratio in Table 11) as previously described for homogeneous Lewis acidic catalytic systems.^[116]

The highest conversions are achieved with supported metal triflates (Table 11, entries 12-14), sulfonated mesoporous silica (Table 11, entry 10) and Amberlyst 15.

Nafion NR 50 (Table 11, entry 1) another sulfonated resin, gave, instead, slightly lower conversion but higher selectivity than Amberlyst 15 due to its lower acidity (0.8 mmol/g).

Table 11. Glycidol etherification with ethanol in the presence of heterogeneous catalysts.

Entry	Catalyst	Conversion [%]	Selectivity to MAGEs [%]	a/b ratio [%]
1	Nafion NR 50	57	94	77/23
2	M-K10	60	67	85/15
3	Amberlyst 15	91	33	74/26
4*	AC	12	99	n.d.
5*	Naked silica	29	66	n.d.
6*	MPS	33	95	n.d.
7	AC-SO ₃ H	13	98	83/17
8	Naked silica-SO ₃ H-(B)	58	91	76/24
9	MPS-SO ₃ H-(A)	4	99	n.d.
10	MPS-SO ₃ H-(B)	80	87	63/37
11	GO	5	99	n.d.
12 [§]	Al(OTf) ₃ -MPS	94	89	72/28
13 [§]	Bi(OTf) ₃ -MPS	74	88	77/23
14 [§]	Fe(OTf) ₃ -MPS	72	94	65/35

Reaction conditions: 1.0 mL of glycidol (15 mmol), 8 mL of ethanol (135 mmol), 10 wt % of catalyst, 80 °C, 300 rpm, inert atmosphere, 1 h; * reaction time of 24 h; § metal triflate loading of 0.01 % in moles (determined by ICP-OES). n.d.: not detected.

Silica sulfonated with chlorosulfonic acid (Naked silica-SO₃H-(B) and MPS-SO₃H-(B)) are more acid and so more active than the one sulfonated with sulfuric acid (Table 11, entry 8-9-10).

Graphene oxide (GO) and sulfonated charcoal produce selectively MAGEs but with low productivity due to their lower acidity (Table 11, see entries 11 and 5). On the contrary, Montmorillonite-K10 (M-K10) reaches a moderate glycidol conversion but a low selectivity to MAGEs, due to glycidol oligomerization (Table 11, entry 2).

Amberlyst 15 gave the lowest selectivity to MAGEs (Table 11, entry 3) probably due to its high acidity (4.7 mmol/g) that favors side reactions as reported in literature for similar compounds.^[117]

In order to evaluate the interaction between glycidol and the sulfonic moieties of this resin, combined ^{13}C -NMR experiments (Magic angle spinning or MAS solid state) were performed on Amberlyst 15 before and after the interaction with glycidol in alcoholic solution (under the same condition used for the catalytic screening).

It is worth noting that two broad peaks are present on MAS ^{13}C -NMR spectrum of commercial Amberlyst 15 (Figure 39 a), one corresponding to the aliphatic chain carbons (45 ppm) and another one to those of the aromatic ring carbons (130 ppm). After the interaction with glycidol (Figure 39 b), two new peaks appear at 63 and 74 ppm, not ascribable to glycidol itself.

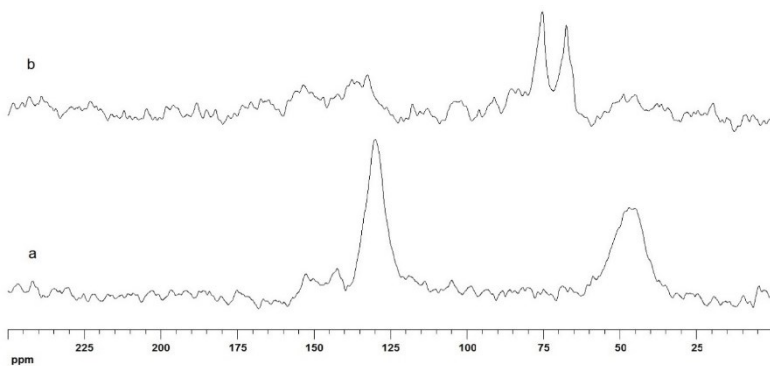


Figure 39. Comparison of ^{13}C -NMR spectra of Amberlyst 15 before (a) and after (b) reaction.

Considering these results, the formation of a covalent bond between glycidol and Amberlyst 15 was hypothesized (Figure 40).

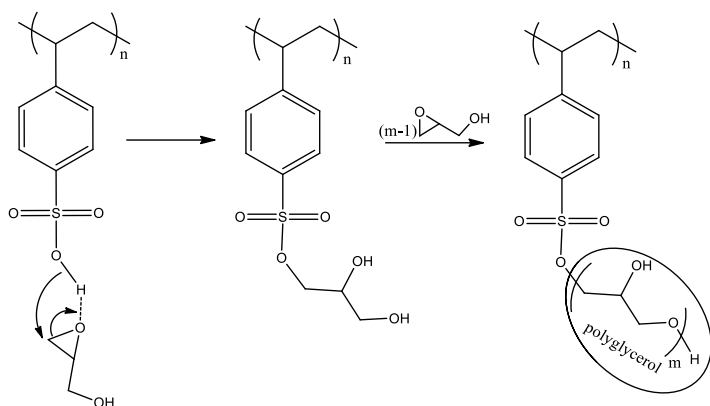


Figure 40. Interaction between glycidol and Amberlyst 15.

Likely, the acidic sulfonic groups of the resin react with activated molecules of glycidol to form intermediates that can interact with others glycidol molecules to give glycidol oligomers linked to the sulfonated moieties of the resin, displaying typical signals of polyglycerol in the NMR spectrum reported in Figure 39 b.

With the aim of selecting the best heterogeneous catalytic system, tests of recyclability were performed by using the most active and selective catalysts (supported metal triflates, MPS-SO₃H-(B) and Nafion NR 50).

After the reaction, the spent catalysts were removed by filtration, washed with ethanol, dried overnight at room temperature and then reused in the reaction of glycidol with ethanol.

Sulfonated silica and supported metal triflates recovered after the first run, were inactive in the etherification of glycidol due to the leaching of all the active species loaded on the supports.

Moreover, supported metal triflates have shown in the first run the same results of the homogeneous ones, confirming this hypothesis.

Nafion NR 50 recycled, instead, maintained the same performances of the fresh catalyst (56 % of conversion and 94 % of selectivity to MAGEs).

3.5.2 Nafion NR 50 as efficient heterogeneous acid catalyst

In light of the obtained results, Nafion NR 50 was preferred as efficient catalyst for glycidol etherification with ethanol. This resin has also been widely employed in sustainable catalytic processes reported in literature.^[118]

In order to find the ideal reaction conditions for this catalytic system, the effect of temperature, alcohol/glycidol molar ratio and catalyst loading on the reaction was evaluated.

The reaction was carried out at 60 °C and 100 °C using a Nafion NR 50 loading of 10 wt %, and an alcohol/glycidol molar ratio of 9.

After 3 h of reaction, only 64 % of conversion was observed at 60 °C with a selectivity of 96 %, while quantitative conversion of glycidol was achieved at 100 °C with a concomitant unwanted formation of considerable amounts of oligomers (79 % of selectivity to ethoxy glyceryl ethers).

Subsequently, the ethanol/glycidol molar ratio was changed from 9:1 to 5:1 and 3:1, performing the reaction at 80 °C for 1 h in the presence of 10 wt % of Nafion NR 50. The conversion increases up to 70 % for a ratio of 5:1 and 90 % for a ratio of 3:1, while the selectivity to ethoxy glyceryl ethers decreases to 85 % and 83 % respectively.

Finally, increasing the catalyst loading to 20 wt %, total conversion was reached in 2 h but a moderate loss of selectivity (89 %) was observed, whereas reducing the catalyst loading to 5 wt %, total conversion of glycidol was achieved after 5 h of reaction with a selectivity to MAGEs of 83 %.

Therefore, the best optimized reaction conditions with Nafion NR50 as heterogeneous catalyst were reached: 80 °C, alcohol/glycidol moles ratio of 9 and a loading of 10 wt %.

Under these conditions, the influence of the reaction time on conversion and selectivity was evaluated as shown in Figure 41.

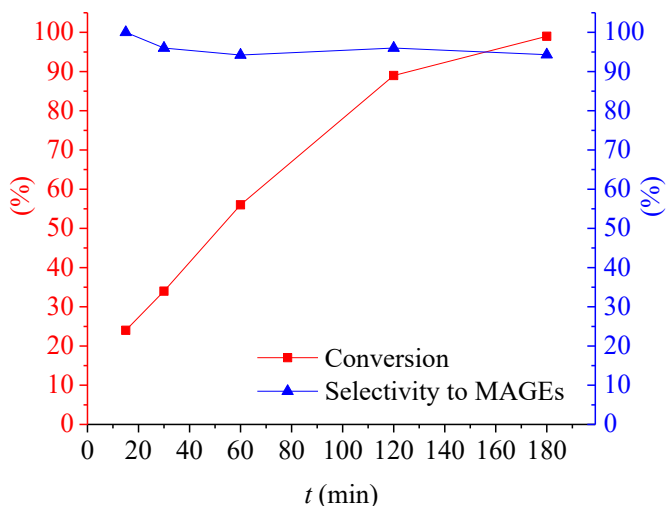


Figure 41. Glycidol etherification with ethanol catalyzed by 10 wt % of Nafion NR 50.

After 15 minutes, a conversion of 24 % was achieved and it gradually raise up to quantitative conversion of glycidol after only 3 h of reaction.

The selectivity to monoethoxy glyceryl ethers remains quite the same during the overall reaction profile, reaching a high value (94 %).

Moreover, monoethoxy glyceryl ether was quantitatively isolated removing the excess of ethanol under reduced pressure (isolated yield of 94 %).

3.5.2.1 Applicability with different alcoholic substrates

Nafion NR 50 was applied as catalyst for the reaction several alcoholic substrates using a loading of 10 wt % at 80 °C (Table 12).

Table 12. Glycidol etherification with different alcohols in the presence of 10 wt % of Nafion NR 50.

Entry	-R	Conversion [%]	Selectivity to MAGEs [%]	a/b ratio [%]
1*	methyl	85	93	77/23
2*	ethyl	57	94	77/23
3	<i>iso</i> -propyl	95	91	78/22
4	<i>tert</i> -butyl	24	73	90/10
5	<i>n</i> -butyl	39	95	72/28
6	<i>iso</i> -butyl	36	90	n.d.
7	<i>n</i> -pentyl	28	92	86/14
8	<i>iso</i> -pentyl	32	98	80/20
9	<i>n</i> -octyl	17	95	n.d.
10	<i>iso</i> -octyl	6	99	n.d.
11	benzyl	65	70	76/24

Reaction conditions: 1.0 mL of glycidol (15 mmol), 135 mmol of alcohol, Nafion NR 50 loading of 10 wt %, 80 °C, 300 rpm, 15 h; * reaction time of 1 h; n.d.: not detected.

The highest conversions and selectivities were achieved with short chain alcohols such as methanol and ethanol in only 1 h of reaction.

As one can see from Table 12, a reduction of conversion was observed increasing the length and the steric hindrance of the alcoholic chain.

High selectivity was achieved for all the alcoholic substrates tested except for *tert*-butanol and benzyl alcohol (Table 12 entry 4 and 11) due to the formation of higher amount of glycidol oligomers probably favored by the different interaction of these substrates with the catalyst.

For alcohols with a longer chain, 15 h of reaction were necessary to reach satisfactory glycidol conversions. Moreover, the a/b ratio increased with the alcoholic alkyl chain length and branching.

3.5.2.2 Catalyst recyclability

Finally, we investigate the catalyst (Nafion NR 50) recyclability under the optimized reaction conditions (80 °C, alcohol/glycidol moles ratio of 9 and a loading of 10 wt %) using ethanol as nucleophile.

After every run of the reaction of glycidol with ethanol, the catalyst was recovered from the reaction mixture by filtration, washed with ethanol, dried overnight at room temperature prior to be reused.

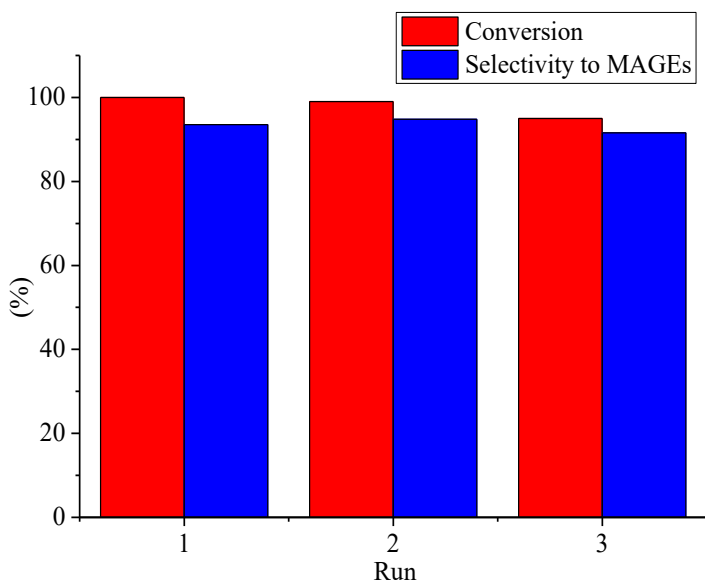
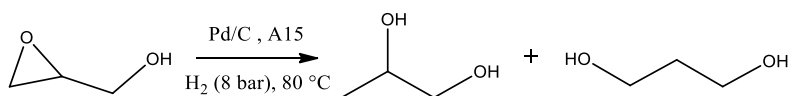


Figure 42. Recyclability of Nafion NR 50 in the etherification reaction.

As shown in Figure 42, Nafion NR 50 is stable and retains high efficiency in the etherification of glycidol with ethanol during three consecutive cycles.

3.6 Amberlyst 15 as co-catalyst for hydrogenolysis of glycidol

Based on the results previously reported in literature regarding the hydrogenolysis of glycidol catalyzed by palladium on carbon (Pd/C)^[80], I have investigated the reaction adding a co-catalyst such as Amberlyst 15 on the reaction medium in order to improve the performances of the catalytic system (Scheme 5).



Scheme 5. Reaction scheme for glycidol hydrogenolysis.

An acid resin like Amberlysty 15, can activate the epoxide towards the ring opening thus favouring the hydrogenolysis reaction.

3.6.1 Screening of the experimental conditions

Starting from the optimized reaction conditions previously reported^[80], the reactions were performed at 80 °C, under a hydrogen pressure of 8 bar, using 10 wt % of a Pd/C catalyst (loaded with 10 wt % of Pd) respect to glycidol varying the amount of Amberlyst 15 from 0.1 to 10 wt %.

Moreover, a solvent was added to the reaction medium to limit glycidol oligomerization. In particular, runs were carried out using ethanol (Table 13) and tetrahydrofuran (Table 14), already identified as good solvents for this reaction.^[80]

Table 13. Glycidol hydrogenolysis in ethanol.

Entry	A15 [wt %]	Conversion [%]	Selectivity to 1,2-PD [%]	Glycidol on A15 [%]*
1	1	100	77	/
2	5	97	68	14
3	10	98	40	44

Reaction conditions: 0.1 g of 10 %wt Pd/C, 80 °C, 1 mL of glycidol, 8 bars H₂, 5 mL ethanol, 1 h. *represents the amount of glycidol linked to A15 resin.

As we can see from Table 13, total conversion of glycidol was achieved after only 1 h of reaction at 80 °C, using ethanol as solvent, with all the amount of Amberlyst 15 tested.

The hydrogenolysis reaction occurs with total selectivity to 1,2-propanediol, in fact no formation of 1,3-propanediol was detected. However, the overall selectivity toward 1,2-propanediol is very low, due to the formation of some by-products that not originate from the hydrogenolysis reaction. Moreover, the amount of these by-products increases with the raise of Amberlyst 15 loading.

Actually, two types of side reactions take place:

- 1) the formation of ethoxy glyceryl ethers through the reaction of glycidol with ethanol favored by the presence of Amberlyst 15;
- 2) the formation of glycidol oligomers that remain covalently linked to the resin as previously described.

Replacing ethanol with tetrahydrofuran as solvent^[119], the formation of glycerol ethers can not take place and total selectivity to propylene glycol is achieved using Amberlyst 15 loading from 0.1 to 1 wt % as we can see from Table 14.

Table 14. Glycidol hydrogenolysis in THF.

Entry	A15 [wt %]	Conversion [%]	Selectivity to 1,2-PD [%]	Glycidol on A15 [%]*
1	0.1	78	100	/
2	0.5	80	100	/
3	1	100	100	/
4	5	97	68	32
5	10	98	50	50

Reaction conditions: 0.1 g of 10 wt % Pd/C, 80 °C, 1 mL of glycidol, 8 bars H₂, 5 mL THF, 1 h. *represents the amount of glycidol linked to A15 resin.

At a highest Amberlyst 15 loading, a reduction of the selectivity to 1,2-PD was observed due to the interaction between glycidol and A15 as described above.

Thus, the best conversion and selectivity was achieved using 1 wt % of Amberlyst 15 as co-catalyst and tetrahydrofuran as solvent.

These results are consistent with those reported in literature^[117], since the optimization of the best Pd/C and A15 mass ratio is crucial for this type of acid/hydrogenating catalytic pathway to enhance the reaction selectivity.

Moreover, the effect of the reaction time was studied under the optimized reaction conditions (80 °C, hydrogen pressure of 8 bars in THF, using Pd/C and 1 wt % of A15) in the time range 15-60 minutes.

As evidenced in Figure 43, the glycidol conversion increases up to 100 % after 1 h while high selectivity to 1,2-PD is retained (> 99 % in all cases).

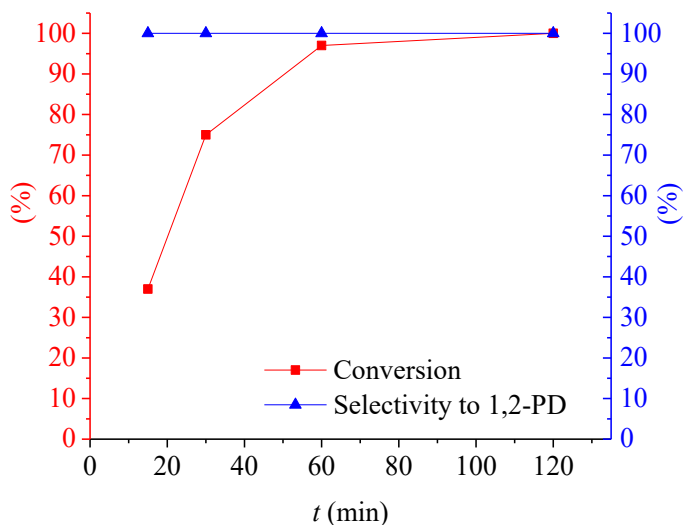


Figure 43. Glycidol conversion using Pd/C-A15 and THF as solvent.

Accordingly, the use of A15 as co-catalyst allows to improve the performances of the catalytic systems reducing the reaction time (1 h respect to 6 h for a total conversion) and consequentially increasing the TOF value, calculated after 30 min, from 27 h⁻¹ (using only Pd/C) to 162 h⁻¹ (for the binary system Pd/C-A15).

3.6.2 Recyclability tests of the catalytic system

The catalytic system (10 wt % Pd/C-A15) was tested for several consecutive catalytic cycles to verify its recyclability.

During seven consecutive catalytic cycles (Figure 44), the catalyst maintained good conversion (about 90 %) and high selectivity to 1,2-PD (98 %) with a reduction of the conversion only at seventh cycle (65 %).

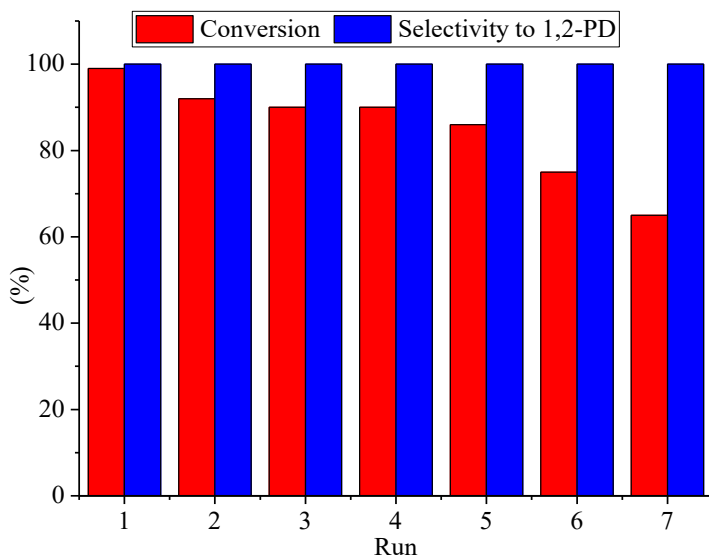


Figure 44. Recyclability of Pd/C-A15 catalyst.

Moreover, a reactivation process for the deactivated catalytic system was carried out using a literature methodology.^[120]

The reactivated catalyst gave the products with a total selectivity to 1,2-propanediol and a conversion of 75 %, with a moderate increase compared to the seventh cycle (65 %).

Finally, this catalytic system composed of Pd/C and Amberlyst 15 has a recyclability very close to that of Pd/C alone (stable for ten catalytic cycles). This approach allowed us to reduce the reaction time from 6 to 1 hour by adding a low price commercially available resin instead of increasing the amount of a noble metal such as Pd.

3.6.3 Characterization of the catalytic system after the reaction

In order to better understand the mechanism involved in the catalysis and in the deactivation, the catalytic system (10 wt % Pd/C-A15) was analyzed before and after hydrogenolysis reactions using different techniques.

Energy dispersive X-ray (EDX) spectrum (Figure 45) has shown that the amount of Pd is the same in different point of a particle and among all the particles.

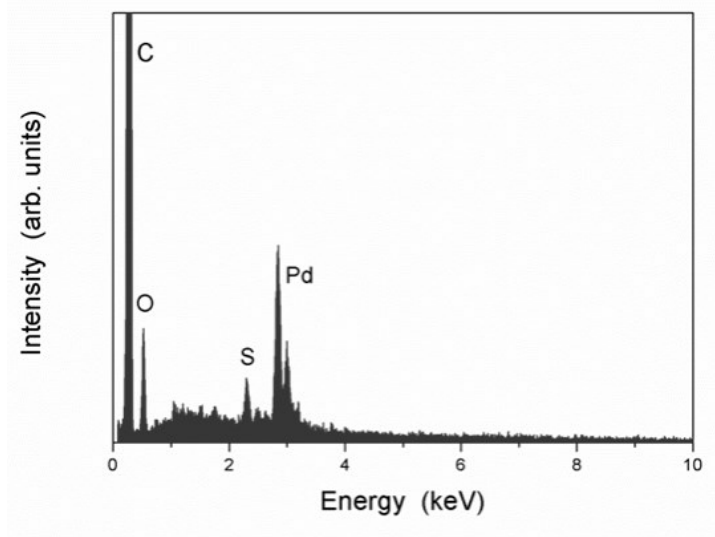


Figure 45. EDX spectra of Amberlyst 15 and Pd/C mixed powder.

X-ray diffraction (XRD) measurements were performed on Pd/C (10 wt %), Amberlyst 15, and the catalytic system (Pd/C-A15) before and after seven catalytic cycles (Figure 46).

The spectrum of the fresh catalyst (Pd/C-A15) is quite similar to that of Pd/C alone, showing characteristic peaks for palladium at $2\theta = 40.2^\circ$ and 68.4° that correspond to Miller indices (111) and (220) and others signals attributed to activated charcoal and palladium oxide ($2\theta = 34.2^\circ$ and 43.4°).^[121]

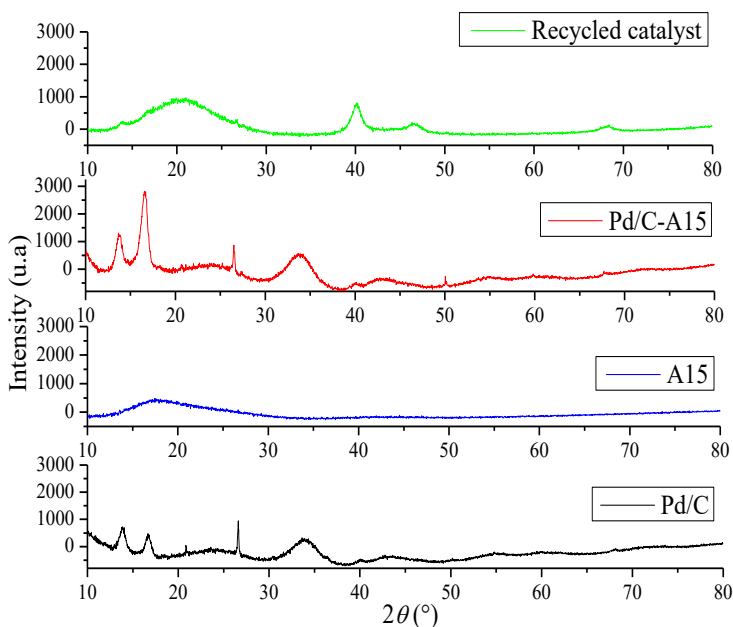


Figure 46. XRD patterns of 10 wt % Pd/C, A15, 10 wt % Pd/C-A15 before and after seven catalytic cycles.

After seven consecutive catalytic cycles, the occurrence of a new signal at $2\theta = 47.5^\circ$ corresponding to the (200) plane diffraction pattern of palladium, attests the reduction of Pd(II) to Pd(0) under catalysis.

These results are in line with that of X-ray photoelectron spectroscopy (XPS) analyses in which the fresh catalyst shows typical peaks of Pd(II) (Figure 47 a and b) that after seven catalytic cycles is reduced to Pd(0) (Figure 47 c).

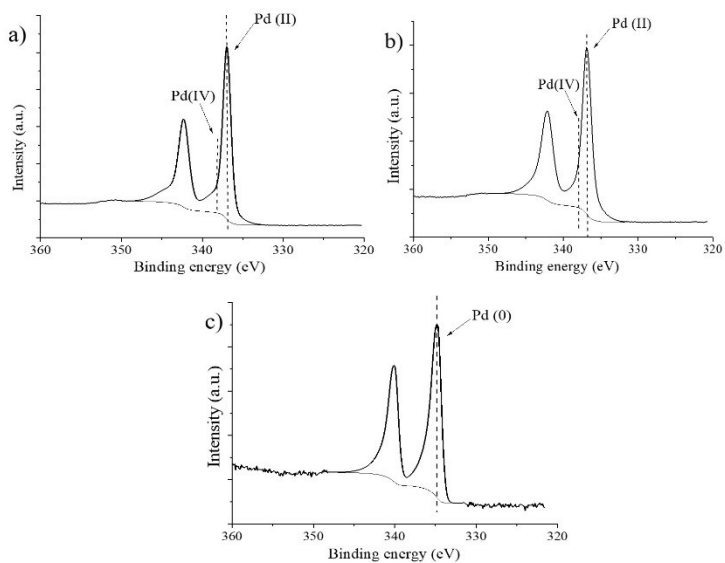


Figure 47. Catalyst Pd/C (a), catalytic system composed by Pd/C and Amberlyst-15 resin (b) and catalytic system used several times in the hydrogenation reaction (c).

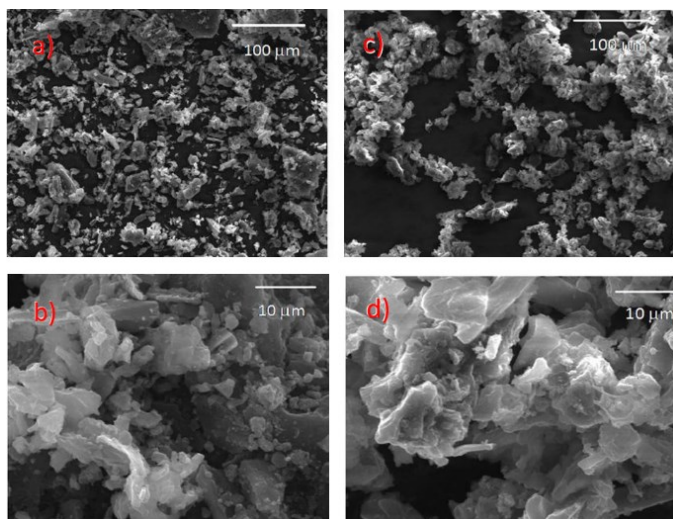


Figure 48. SEM images of powder of Amberlyst 15 and catalyst (Pd/C-A15): a) and b) before reaction, c) and d) after reaction.

Scanning electron microscope (SEM) images (Figure 48) were recorded for the catalytic system, composed of Pd/C and Amberlyst 15 powdered and mixed.

The particles size of the fresh catalytic system ranges from 1 to 100 μm (Figure 48 a and b), after the hydrogenolysis reaction (Figure 48 c and d), instead, the particles distribution is more homogeneous.

Transmission electron microscopy (TEM) image of the Pd/C-A15 catalyst before and after the reaction are shown in Figure 49.

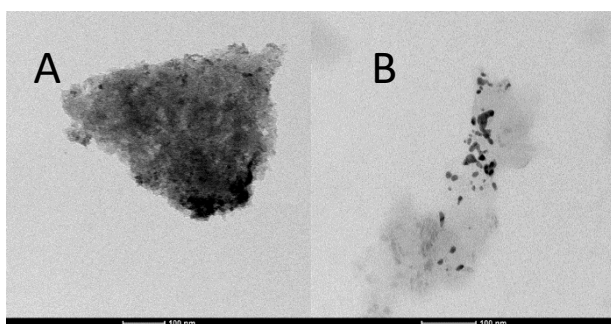


Figure 49. TEM micrograph of the catalyst before (A) and after (B) glycidol hydrogenolysis.

It is worth noting that the morphology completely changes due to the hydrogenolysis reaction.

In fact, the fresh catalyst (Figure 49 a) show nanoparticles of Pd (~10 nm) well distributed in huge agglomerates originated from the polymeric bulk of the resin. After the reaction (Figure 49 b), Pd nanoparticles are large and non-spherical with dimension in the range 15-50 nm.

This phenomenon is probably due to the growth and/or coalescence of the Pd nanoparticles obtained from the reduction of residual Pd(II) salts used as nanoparticles precursors.

Based on these results, the deactivation of the catalyst can be attributed to an irreversible metal nanoparticles aggregation and not to the inactivation of its surface due to a deposition of organic residue.

3.6.4 Environmental considerations

Finally, the innovative glycidol-based route was compared with the industrial fossil-based one, that is the hydration of propylene oxide (Figure 50).

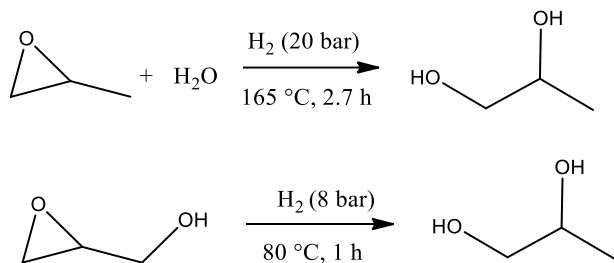


Figure 50. Comparison of 1,2-propanediol synthesis from propylene oxide and glycidol.

The results show that the bio-based process presents an improvement for all the parameters considered such as differences in temperature (in °C), pressure (in bar) and reaction time (in hours).

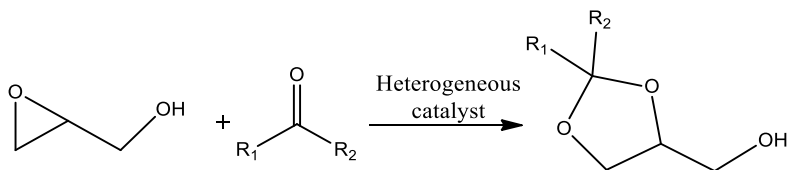
In fact, the reaction temperature is reduced of 52 % with an estimated methane saving of 11 kg. The pressure is also decreased of 60 % (12 bar), and the saved quantity could be used for other purposes (e.g. to inflate up to more than 5 tires).

Furthermore, the reaction time is reduced of 64 % giving a sensible reduction in the operation costs estimated over 87 € per cycle.

3.7 Heterogeneous catalysis for glycidol ketalization

The reaction of glycidol with ketones to produce cyclic ketals was investigated using heterogeneous acid as catalysts (Scheme 6).

Firstly, the catalytic runs were performed using acetone as ketone with a acetone/glycidol molar ratio of 43, heating the system to reflux, as reported in literature for glycidol acetalization in homogeneous phase.^[122]



Scheme 6. Reaction of glycidol with ketones.

In these conditions, acetone acts both as reagent and reaction solvent, avoiding the need of any other organic solvent, finally simplifying the purification of the products and acetone recovery and recycle.

3.7.1 Screening of commercial and synthetic catalysts

A screening of different heterogeneous catalysts (both Lewis and Brønsted acids) was performed for glycidol ketalization to solketal using a catalyst loading of 10 wt % with respect to glycidol (Table 15).

Table 15. Glycidol conversion to solketal in the presence of heterogeneous catalyst.

Entry	Catalyst	Conversion [%]	Selectivity to Solketal [%]
1	Al(OTf) ₃ -MPS	100	93
2	Fe(OTf) ₃ -MPS	100	87
3	Bi(OTf) ₃ -MPS	100	86
4	Amberlyst 15	100	8
5	Nafion NR 50	90	88
6	No catalyst	0	-

Reaction conditions: 350 μ L of glycidol, 15 mL of acetone, reflux, 24 h, 10 wt % of catalyst loading.

Using Montmorillonite K10, sulfonated activated charcoal (AC-SO₃H) and sulfonated mesoporous silica (MPS-SO₃H-(A)) as catalyst, no reaction took place due to their low total acidity as previously reported.

As we can see from Table 15, solketal was obtained with high glycidol conversion and selectivity using both Lewis (metal triflate supported catalyst) and Brønsted (Nafion NR 50) heterogeneous acid catalysts after 24 hours of reaction. By using Amberlyst 15 as catalyst, instead, a drastic reduction of the selectivity is observed due to a glycidol oligomerization as reported for the other reactions studied.

In order to find the best catalytic system, runs were carried out by using catalysts (Nafion NR 50 and supported metal triflates) recovered after the reaction.

No products formation was observed in the presence of supported metal triflates due to the leaching of the active Lewis acid sites under the reaction conditions, as reported in literature for Al(OTf)₃ on mesoporous silica.^[123]

On the contrary, Nafion NR 50 maintains high conversion (90 %) and selectivity to solketal (85 %), proving again to be the best heterogeneous catalytic system for glycidol transformation in value-added products.

3.7.2 Optimization of the reaction conditions with Nafion NR 50

The effect of the temperature, catalyst loading and acetone/glycidol molar ratio was evaluated using the best catalyst, Nafion NR 50.

With the aim of reducing the reaction temperature, runs were also performed at room temperature with a catalyst loading of 10 wt %. However, under these conditions, only 24 % of conversion with a very low selectivity to solketal (50 %) was obtained after 24 h of reaction.

Using a lower catalyst loading such as 5 wt %, after 24 h only 58 % of glycidol conversion was achieved with a total selectivity to solketal.

Increasing the catalyst loading to 20 wt %, instead, allow us to reach total glycidol conversion and selectivity to solketal after 18 h of reaction as we can see from Figure 51.

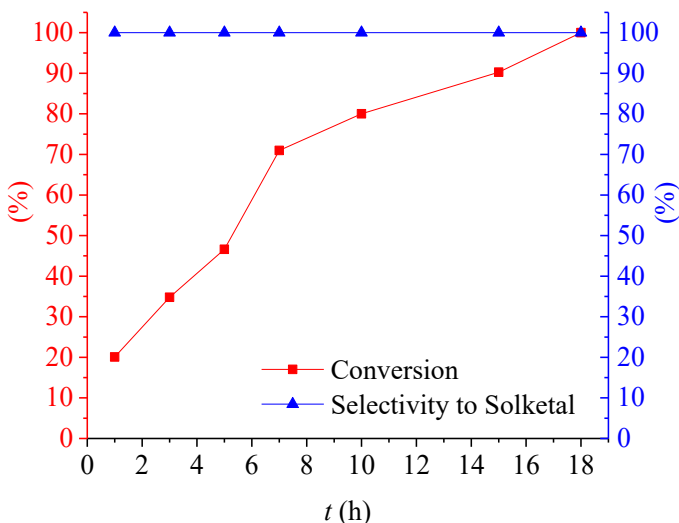


Figure 51. Glycidol conversion to solketal using Nafion NR 50 (20 wt %).

Moreover, a decrease of selectivity to solketal (80 %) was observed reducing the acetone/glycidol ratio to 20:1 using a catalyst loading of 20 wt % under reflux for 18 h, due to a favoured glycidol oligomerization.

Finally, Nafion NR50 promotes the total glycidol conversion to solketal in 18 h using a catalyst loading of 20 wt % under reflux condition with total selectivity to the desired product.

Furthermore, the ketalization of glycidol was investigated using others two ketones such as methylethylketone and 2-pentanone.

Reaction were performed under reflux, using a glycidol/ketone in moles ratio of 43, and a Nafion NR50 loading of 20 wt %.

Glycidol is favourably converted into the corresponding ketals in both cases with high yields, and glycidol oligomers were observed as by-products (12-18 %) (Figure 52).

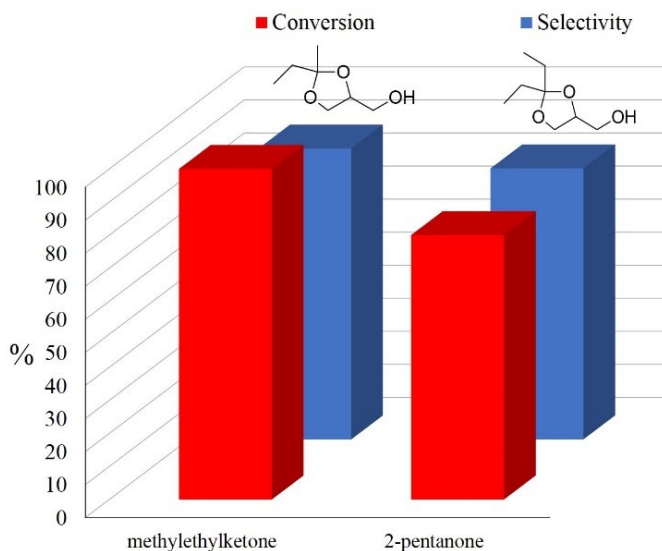


Figure 52. Glycidol ketalization with methylethylketone and 2-pentanone catalysed by Nafion NR 50 (20 % wt).

These substrates have been chosen since the corresponding products of the reaction with glycidol can be used as building blocks to prepare high-value products such as monoalkyl glyceryl ethers.^[89]

3.7.3 Nafion NR 50 recyclability tests

After the reaction under the optimized conditions (glycidol/acetone moles ratio 1:43, catalyst loading of 20 wt %, reflux, 18 h), Nafion NR 50 is recovered from the reaction mixture and washed with fresh acetone (10 mL). Then, it was dried overnight at 40 °C and reused as catalyst for the ketalization of glycidol.

Results show that the catalyst is stable under these conditions and retains high performances during four consecutive cycles (Figure 53).

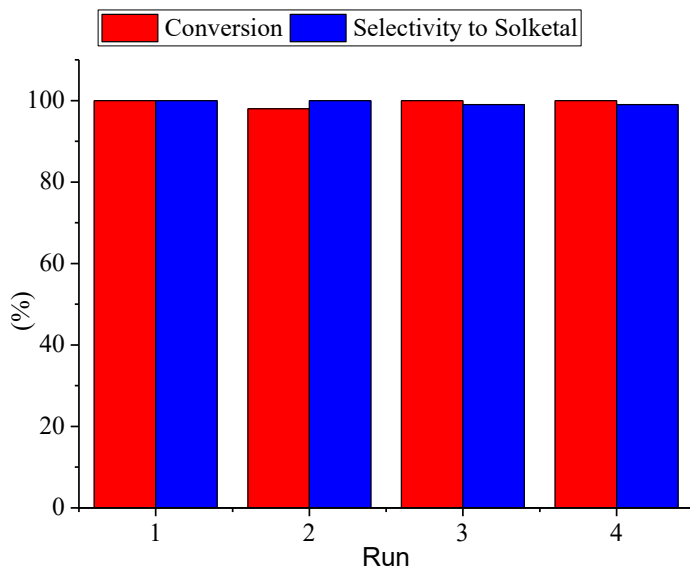


Figure 53. Nafion NR 50 recyclability in glycidol ketalization.

Moreover, the excess acetone used in the reactions was recovered and analysed by GC-FID. These analyses have demonstrated that such acetone has a purity that allow it to be reused in further reactions.

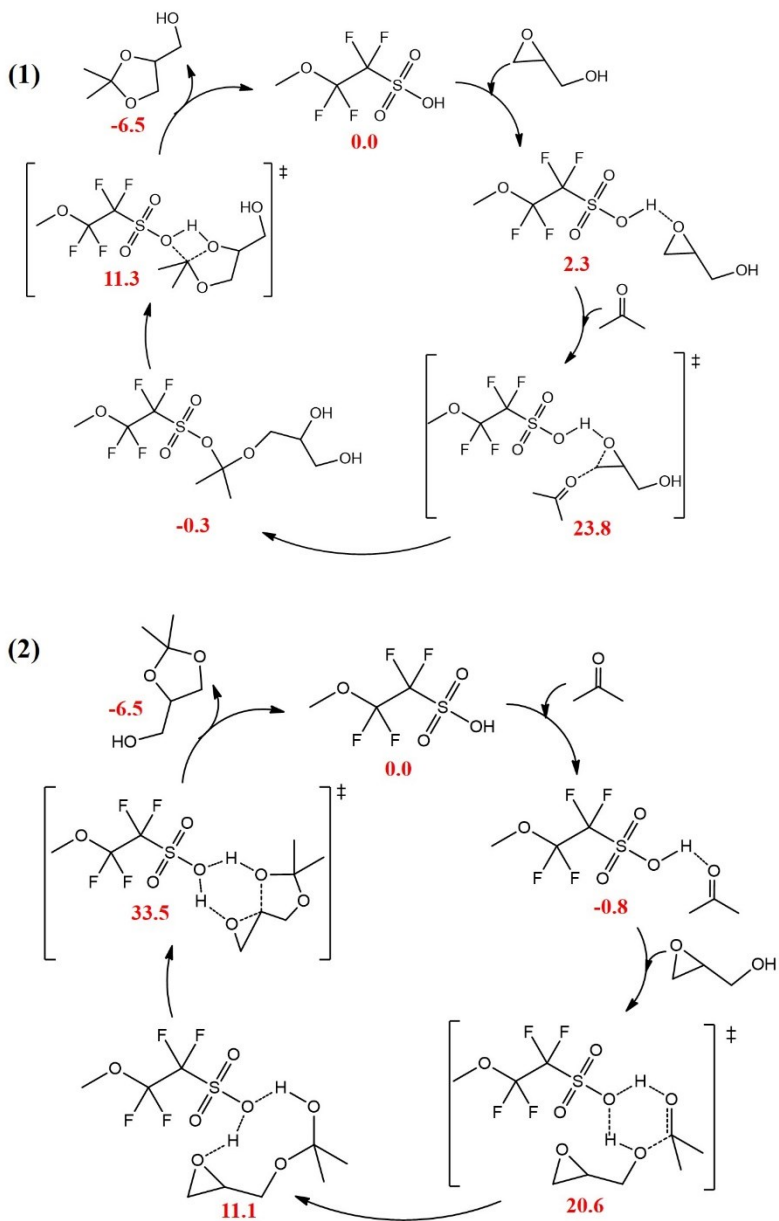
It is important to point out that this aspect is fundamental for the industrial implementation, in fact, the possibility to recycle a solvent increases the sustainability of the overall process, reducing the costs and environmental impact.^[124]

3.7.4 Mechanistic considerations

DFT calculations were performed to study the mechanism of the reaction between glycidol and acetone catalyzed by Nafion NR 50.

In Figure 54 are shown two possible mechanism that have been investigated.

$\Delta G(\text{kcal/mol})$



The first one (1) involves the coordination of the epoxide to the sulfonic moieties of the catalyst through a hydrogen bond, and a subsequent ring opening of epoxide by nucleophilic attack of carbonylic oxygen of acetone.

In the second one (2), instead, acetone was activated by the catalyst towards the nucleophilic addition of the -OH group of glycidol and then occurs the ring opening of the epoxide group.

DFT results show that the favored mechanism is the first one, in which the rate determining step is the ring opening of the epoxide by the nucleophilic attack of the ketone, followed by an easier formation of the five-member ring to give solketal, in line with a mechanism proposed in literature for the same reaction in the presence of an homogeneous catalyst.^[86]

According to the scheme in Figure 55, another product can be formed under these conditions such as 2,2-dimethyl-1,3-dioxan-5-ol, the corresponding six term ring product. From the kinetic point of view, this is the favored product thanks to a most favorable geometry of the ring closing transition state (almost 6 kcal/mol lower).

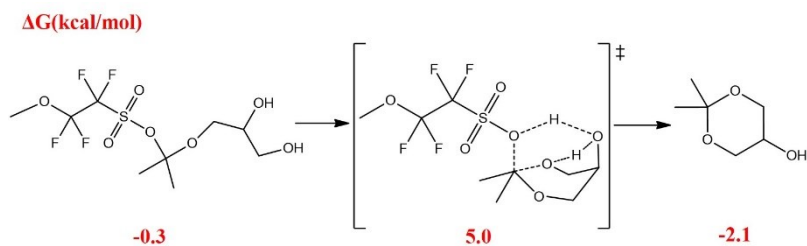


Figure 55. Formation of 2,2-dimethyl-1,3-dioxan-5-ol.

However, solketal is about 5 kcal/mol more stable than 2,2-dimethyl-1,3-dioxan-5-ol, and was obtained as the thermodynamic product of the reaction.

In order to validate the proposed mechanistic considerations, reactions were carried out at lower conversion.

Under the optimized conditions (glycidol/acetone moles ratio 1:43, catalyst Nafion NR 50 loading of 20 wt %, reflux), reactions were conducted for 1h and, after removing the catalyst by filtration, and acetone by using a rotary evaporator, the reaction products were analysed by ^1H and ^{13}C NMR.

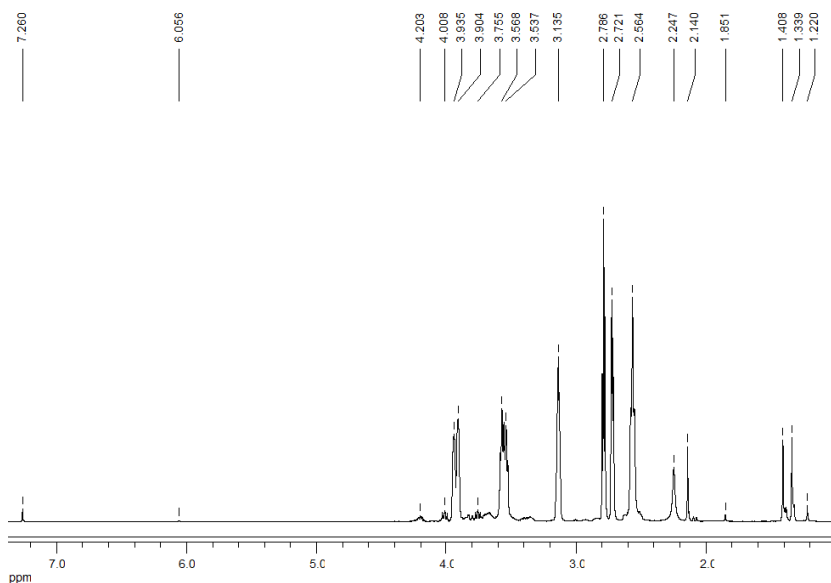


Figure 56. ^1H -NMR (CDCl_3 , 400 MHz) spectrum of reaction mixture.

^1H -NMR spectrum (Figure 56) clearly shows the formation of solketal (characteristic singlet at 1.3 and 1.4 ppm; three doublets of doublets from 4.0 to 3.5 ppm and one multiplet at 4.2 ppm) in the presence of 80 % of unreacted glycidol (doublet of doublets at 3.9 ppm, doublet of doublets 3.6 ppm, multiplet at 3.5 ppm, doublet of doublets at 3.1 ppm, doublet of doublets at 2.8 ppm, doublet of doublets at 2.7 ppm and triplet at 2.6 ppm).

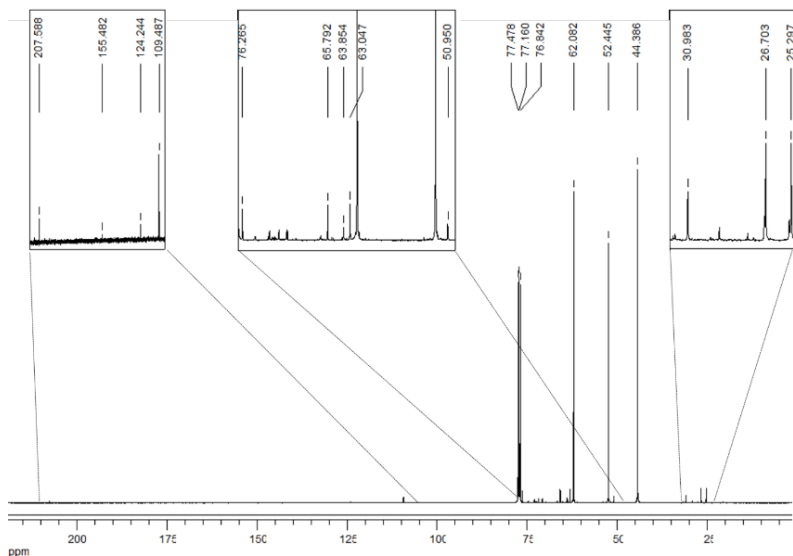


Figure 57. ^{13}C -NMR (CDCl_3 , 100 MHz) spectrum of reaction mixture.

^{13}C -NMR spectrum (Figure 57) confirms the presence of solketal (109.5, 76.3, 65.8, 63.0, 26.7 and 25.3 ppm) and glycidol (62.1, 52.4 and 44.4 ppm).

Characteristic signal of 2,2-dimethyl-1,3-dioxan-5-ol was not observed to the rapid isomerization of this compound to solketal, the more stable isomer as confirmed by DFT calculations. The other signals observed was attributed acetone impurities (207.6 and 30.98 ppm at ^{13}C and 2.14 ppm at ^1H) and to the products of aldolic condensation of acetone (4-hydroxy-4-methylpentan-2-one and mesityl oxide), in the presence of an acidic heterogenous catalyst such as Nafion, that don't affect the reaction yield. Additional calculations were performed for the reaction in the presence of an inactive catalyst such as sulfonated silica in order to find an explanation for the higher performances showed by Nafion NR 50 respect to the other heterogeneous catalytic systems tested.

For sulfonated silica, the rate determining step has a barrier almost 4.5 kcal/mol higher than for the Nafion NR 50.

In the light of these results, the higher activity of Nafion NR 50 was imputed to the higher acidity of its sulfonic groups that are more able to activate the epoxide towards the nucleophilic attack of the ketone, resulting in a higher reaction yield.

3.8 References

- [108] X. Bi, X. Ren, Z. Huang, M. Yu, E. Kreidler, Y. Wu, *Chem. Commun.* **2015**, 51, 7665–7668.
- [109] E. Nasybulin, W. Xu, M. H. Engelhard, Z. Nie, S. D. Burton, L. Cosimbescu, M. E. Gross, J.-G. Zhang, *J. Phys. Chem. C* **2013**, 117, 2635–2645.
- [110] J. F. Knifton, J. R. Sanderson, M. E. Stockton, *Catal. Lett.* **2001**, 73, 55–57.
- [111] S. Casati, P. Ciuffreda, E. Santaniello, *Tetrahedron Asymmetry* **2011**, 22, 658–661.
- [112] S. F. Martin, J. A. Josey, Y.-L. Wong, D. W. Dean, *J. Org. Chem.* **1994**, 59, 4805–4820.
- [113] H. Aitchison, R. L. Wingad, D. F. Wass, *ACS Catal.* **2016**, 6, 7125–7132.
- [114] F. Jérôme, Y. Pouilloux, J. Barrault, *ChemSusChem* **2008**, 1, 586–613.
- [115] J.-P. Lange, *ChemSusChem* **2017**, 10, 245–252.
- [116] R. Cucciniello, M. Ricciardi, R. Vitiello, M. Di Serio, A. Proto, C. Capacchione, *ChemSusChem* **2016**, 9, 3272–3275.
- [117] J. Kluczka, T. Korolewicz, M. Zołotajkin, J. Adamek, *Water Resour. Ind.* **2015**, 11, 46–57.
- [118] M. J. Climent, A. Corma, S. Iborra, S. Martínez-Silvestre, A. Velty, *ChemSusChem* **2013**, 6, 1224–1234.
- [119] C. M. Cai, T. Zhang, R. Kumar, C. E. Wyman, *Green Chem.* **2013**, 15, 3140–3145.
- [120] D. L. Sikkenga, I. C. Zaenger, G. S. Williams, *Palladium Catalyst Reactivation*, **1991**, US4999326 A.
- [121] D. Briggs, M. P. Seah, Eds. *Practical Surface Analysis, Auger and X-Ray Photoelectron Spectroscopy*, Wiley, Chichester, **1996**.
- [122] I. Mohammadpoor-Baltork, A. R. Khosropour, H. Aliyan, *Synth. Commun.* **2001**, 31, 3411–3416.
- [123] K. N. Tayade, M. Mishra, M. K. R. S. Somani, *Catal. Sci. Technol.* **2015**, 5, 2427–2440.
- [124] R. Cucciniello, D. Cespi, *Recycling* **2018**, 3, 22.

4 Conclusion

During the three years of my PhD project, I have investigated the catalytic conversion of bio-glycidol into value-added products.

Bio-glycidol was successfully synthesized from a waste of an industrial process (Epicerol®) and employed as starting material to produce glyceryl ethers, propanediols and glycerol ketals.

Monoalkyl glyceryl ethers were efficiently synthesized for the first time by etherification of glycidol catalysed by homogeneous and heterogeneous Lewis and Brønsted acids. Among all the homogeneous catalysts tested, Al(OTf)₃ gave the highest turnover frequencies (until 13400 h⁻¹ at 80 °C), very good selectivity to MAGEs (90 %) but quite low regioselectivity, with a ratio of isomeric ethers (a/b) around 75/25. Excellent regioselectivity (a/b ratio until 96/4), selectivity to MAGEs higher than 95 % and turnover frequencies close to 1200 h⁻¹ are instead obtained using a sterically demanding [OSSO]-type Fe(III) complex with a triflate ion in the coordination sphere. The high regioselectivity reached with this Fe(III) complex is an important aspect to accomplish MAGEs with applications in biological and pharmaceutical fields. MAGEs were prepared with good results also under heterogeneous conditions, that are more appealing for industrial application. In particular, Nafion NR 50, a commercially available sulfonated resin, produced ethoxy glyceryl ethers in 3 h at 80 °C using a catalyst loading of 10 wt %, retaining high efficiency during three consecutive cycles.

Concerning propanediols, 1,2-propanediol was selectively obtained through glycidol hydrogenolysis after 1 h of reaction at 80 °C and 8 bar of H₂ using a catalytic system based on Pd/C and 1 wt % of A15 and THF as solvent.

The addition of Amberlyst 15 allowed to use a lower amount of noble metal and obtain the desired product with good conversion (90-75 %) and high selectivity using the same catalytic system for seven reaction cycles.

Finally, heterogeneous catalysis was applied to produce glycerol ketals through reaction of glycidol with ketones. Nafion NR 50 promoted the quantitative and selective formation of solketal in 18 h under reflux acetone using a catalyst loading of 20 wt % without any loss of activity and selectivity under four reaction cycles.

In conclusion, the proposed routes have some potential advantages, in term of both process efficiency and environmental sustainability as proved by life cycle assessment analyses, performed comparing the data obtained at a laboratory scale using bio-glycidol as starting material with those reported in literature.

Acknowledgments

A conclusione di questi tre anni di Dottorato sento il dovere e il piacere di ringraziare tutte le persone che hanno contribuito al raggiungimento di questo obiettivo.

Innanzitutto, vorrei esprimere la mia profonda gratitudine al Professore Proto per essere stato una guida sempre presente non solo in laboratorio ma anche fuori, per avermi lasciato la libertà di scegliere come impostare la ricerca, per avermi permesso di partecipare a numerosi congressi ma anche per tutte le feste e le gite condivise insieme. Tutto ciò mi ha permesso di crescere come chimico ma soprattutto come persona.

Devo altresì ringraziare il Professore Capacchione per la costante disponibilità e l'aiuto, il Professore Passarini e Daniele per aver arricchito la ricerca grazie alle loro collaborazioni.

Desidero, ringraziare tutto il lab. 8 (Concetta, Adriano, Milo, Ilaria, Raffaele) che in questi tre anni è diventato una vera e propria casa, o meglio una famiglia in cui si condividono le gioie e i dolori.

In particolare, voglio ringraziare Raffaele, il nostro Presidente-Professore, per il suo enorme aiuto in tutto, i consigli, gli incoraggiamenti, la fiducia che ha sempre riposto in me e soprattutto perché senza di lui i risultati ottenuti non sarebbero stati gli stessi.

Un ringraziamento speciale va a Milo sul quale ho potuto fare affidamento sia nei momenti di gioia che in quelli di sconforto nei quali ha sempre cercato di confortarmi e rallegrarmi.

Non posso non ringraziare Ylenia, l'amica che mi ha sempre sostenuto ed aiutato durante questo percorso di crescita, condividendo le gioie e le soddisfazioni, così come le preoccupazioni, aiutandomi a superare i vari momenti di crisi.

Desidero, inoltre, ringraziare Gianmatteo che negli ultimi mesi mi ha supportato e sopportato durante i deliri per la scrittura di questa tesi.

Ringrazio con affetto tutta la mia famiglia e il mio ragazzo Natale che mi hanno sempre sostenuto ed incoraggiato in questi anni nonostante tutto. Tutte queste cose messe insieme hanno reso questi tre anni per me meravigliosi ed indimenticabili.

PUBLICATIONS ON THE PhD PROJECT

- D. Cespi, R. Cucciniello, M. Ricciardi, C. Capacchione, I. Vassura, F. Passarini, A. Proto, “Simplified early stage assessment of process intensifications: glycidol as value-added product from epichlorohydrin industry wastes”, *Green Chem*, **2016**, *18* (16), 4559–4570.
- R. Cucciniello, M. Ricciardi, R. Vitiello, M. Di Serio, A. Proto, C. Capacchione, “Synthesis of Monoalkyl Glyceryl Ethers by Ring Opening of Glycidol with Alcohols in the Presence of Lewis Acids”, *ChemSusChem* **2016**, *9* (23), 3272–3275.
- M. Ricciardi, F. Passarini, I. Vassura, A. Proto, C. Capacchione, R. Cucciniello, D. Cespi, “Glycidol, a Valuable Substrate for the Synthesis of Monoalkyl Glyceryl Ethers: A Simplified Life Cycle Approach”, *ChemSusChem* **2017**, *10*, 2291-2300.
- M. Ricciardi, D. Cespi, M. Celentano, A. Genga, C. Malitesta, A. Proto, C. Capacchione, R. Cucciniello, “Bio-propylene glycol as value-added product from Epicerol® process”, *Sustain. Chem. Pharm.*, **2017**, *6*, 10–13.
- M. Ricciardi, F. Passarini, C. Capacchione, A. Proto, J. Barrault, R. Cucciniello, D. Cespi, “First Attempt of Glycidol-to-Monoalkyl Glyceryl Ethers Conversion by Acid Heterogeneous Catalysis: Synthesis and Simplified Sustainability Assessment” *ChemSusChem* **2018**, *11*, 1829–1837.

- M. Ricciardi, L. Falivene, T. Tabanelli, A. Proto, R. Cucciniello, F. Cavani “Bio-Glycidol Conversion to Solketal over Acid Heterogeneous Catalysts: Synthesis and Theoretical Approach” *Catalysts* **2018**, 8, 391.

CONTRIBUTION TO CONFERENCES

- R. Cucciniello, M. Ricciardi, C. Pironti, O. Motta, A. Proto “The treasure of reaction by-products: from 2-monochlorohydrin to additives for gasoline”, XVI National Congress of environment and cultural heritage Chemistry, Bergamo, Italy, 14-18 June 2015.
- R. Cucciniello, M. Ricciardi, C. Pironti, A. Proto. “Synthesis of fuel additives by conversion of 2-chloro-1,3-propanediol”, Workshop “Chemistry, Environment and Territory”, Caserta, Italy, 30 September 2015. **(Poster)**
- D. Cespi, F. Passarini, I. Vassura, F. Cavani, R. Cucciniello, M. Ricciardi, C. Capacchione, A. Proto, “Evaluation and optimization of chemical processes through a life cycle perspective”, XVI National Congress of environment and cultural heritage Chemistry, Lecce, Italy, 29 June 2016.
- R. Cucciniello, D. Cespi, M. Ricciardi, C. Capacchione, I. Vassura, A. Genga, F. Passarini, A. Proto, “Valorisation of by-products of established industrial processes: glycidol and others value-added products from epichlorohydrin industry wastes” XVI

National Congress of environment and cultural heritage Chemistry, Lecce, Italy, 29 June 2016.

- M. Ricciardi, R. Cucciniello, A. Proto, C. Capacchione, “Glycerol ether synthesis by ring-opening reaction of glycidol with alcohols catalyzed by Lewis acids”, XIX National Congress of Catalysis, Bressanone, Italy, 13 September 2016. (**Oral Presentation**)

- R. Cucciniello, M. Ricciardi, C. Pironti, C. Capacchione, A. Proto, “Preparation of 1,2-propanediol through glycidol hydrogenolysis”, Merck Young Chemists Symposium, Rimini, Italy, 25 October 2016. (**Poster**)

- M. Ricciardi, R. Cucciniello, C. Capacchione, A. Proto, “Synthesis of monoalkyl glyceryl ethers through reaction of glycidol with alcohols in presence of Lewis acids”, Merck Young Chemists Symposium, Rimini, Italy, 26 October 2016. (**Poster**)

- M. Ricciardi, R. Cucciniello, C. Capacchione, A. Proto, “Green synthesis of glycerol monoethers”, NanoMeetsBio@Nanomates, Fisciano (SA), Italy, 16 February 2017. (**Poster**)

- M. Ricciardi, R. Cucciniello, C. Capacchione, A. Proto, “Glycerol ethers synthesis: glycidol route”, 5th National Workshop of Green Chemistry, Roma, Italy, 16 June 2017. (**Flash Presentation + Poster**)

- M. Ricciardi, R. Cucciniello, M. Di Serio, C. Capacchione, A. Proto, “A new sustainable catalytic route to produce monoalkyl

glyceryl ethers using glycidol as feedstock”, EUROPACAT 2017, Firenze, Italy, 28 August 2017. (**Poster**)

- M. Ricciardi, R. Cucciniello, D. Cespi, C. Capacchione, I. Vassura, F. Passarini, A. Proto, “Synthesis of monoalkyl glyceryl ethers using glycidol as green starting material”, XXVI National Congress of Italian Chemical Society, Paestum (SA), Italy, 12 September 2017. (**Flash Presentation + Poster**)
- M. Ricciardi, R. Cucciniello, C. Capacchione, A. Proto, “Monoalkyl glyceryl ethers production in the presence of homogeneous and heterogeneous acid catalysts”, XXVI National Congress of Italian Chemical Society, Paestum (SA), Italy, 13 September 2017. (**Poster**)
- M. Ricciardi, R. Cucciniello, C. Capacchione, A. Proto, “Glycidol as green feedstock for the synthesis of fine chemicals”, Merck Young Chemists Symposium, Milano-Marittima (Ra), Italy, 15 November 2017. (**Oral Presentation**)
- R. Cucciniello, M. Ricciardi, D. Cespi, F. Passarini, C. Capacchione, J. Barrault, A. Proto, “Glycidol as green feedstock in the synthesis of value-added products”, 3rd Green & Sustainable Chemistry Conference, Berlin, Germany, 14 May 2018. (**Poster**)
- M. Ricciardi, A. Proto, C. Capacchione, R. Cucciniello, “Benign-by-design approach for the conversion of by-products into value-added products: glyceryl ethers synthesis from glycidol”, 6th

National Workshop of Green Chemistry, Milano, Italy, 15 June 2018. (**Flash Presentation + Poster**)

- A. Proto, M. Ricciardi, C. Capacchione, J. Barrault, F. Passarini, D. Cespi, R. Cucciniello, “From wastes to value-added products: synthesis of monoalkyl glyceryl ethers as case study”, XVII National Congress of environment and cultural heritage Chemistry, Genova, Italy, 24-27 June 2018.

PRIZES

- Best Flash Presentation at 5th National Workshop of Green Chemistry, Roma, Italy, 16 June 2017.